

Project Number: JAO-0701

**EXPLORING INERTIAL NAVIGATION TECHNIQUES
FOR PRECISION PERSONNEL LOCATION**

A Major Qualifying Project Report

Submitted to the Faculty

of the

WORCESTER POLYTECHNIC INSTITUTE

In Partial Fulfillment of the Requirements for the

Degree of Bachelor of Science

By

Tiffany Warrington

And

Eric Wong

Date: April 24, 2007

Approved:

Professor John A. Orr, Major Advisor

I Abstract

This project aimed at characterizing both MEMs accelerometers and gyroscopes for use in a low cost inertial navigation unit. A hardware and software system, consisting of MEMs sensors, A/D converters, a 200 MHz processor, compact flash memory, and C++ coded software, was integrated into a test bed that calculates and outputs the unit's final positioning after acceleration and/or rotation was applied. Testing of the unit proved that low cost sensors, performing at specifications are unable to provide accurate positioning with the current performance of MEMs technology.

II Acknowledgements

We would like to thank the following people for their help throughout this project:

Professor John A. Orr

Professor Cosme Furlong

Irene Gouverneur

Fred Hutson

Brad A. Miller

Worcester Polytechnic Institute

III Table of Contents

I Abstract.....	2
II Acknowledgements	3
III Table of Contents	4
IV List of Figures	5
V List of Tables.....	6
1 Introduction	7
2 Problem Statement	8
3 Project Goals and Requirements	8
4 Technical Background.....	9
4.1 GPS.....	9
4.2 Dead Reckoning.....	11
4.3 Impulse Ultra-Wide Band	11
4.4 Direction Finding	13
4.5 Inertial Navigation.....	14
4.5.1 Accelerometers.....	15
4.5.2 Gyroscopes	16
4.5.3 Sensor Error.....	20
4.5.4 Magnetometers and Compasses	22
4.6 Potential System Block Diagram	23
4.7 Processing Unit	23
4.8 Memory Storage.....	24
5 Final Design	25
5.1 Physical Parameters.....	26
5.1.1 Sensors	28
5.1.1.1 2-axis Accelerometer ADXL203	28
5.1.1.2 Yaw Rate Sensor Gyroscope ADXRS150	31
5.1.2 Processor	33
5.2 Software	35
5.2.1 Step 1.....	36
5.2.2 Step 2.....	37
5.2.3 Step 3.....	37
5.2.4 Step 4.....	38
5.2.5 Step 5.....	38
5.2.6 Software Changes and Additions	39
5.2.7 Software Validation.....	40
5.3 System Functionality.....	42
5.4 Operational Modes	45
6 Testing and Results	45
6.1 Test Plan.....	46
6.2 Stationary	46
6.3 Rotary Stage Testing.....	53
6.4 One-Dimensional	56
6.5 Two-Dimensional.....	59

6.6	Error Analysis	63
6.7	Sensor Specification Testing.....	68
6.7.1	Accelerometer Zero g Bias Level.....	68
6.7.2	Accelerometer Temperature Variance	69
6.7.3	Accelerometer Sensitivity	70
6.7.4	Gyroscope Zero Rotation Null Value.....	71
6.7.5	Gyroscope Sensitivity	71
6.7.6	Gyroscope Temperature Variance.....	72
6.7.7	Gyroscope Self Test Response.....	73
7	Conclusions	73
8	References	76

IV List of Figures

Figure 1:	GPS Trilateration Methods	10
Figure 2:	Cell phone using GPS Navigation.....	10
Figure 3 -	Bandwidth of Signal Types	12
Figure 4:	Solenoid and Directional Antenna.....	13
Figure 5:	Three dimensional axis.....	14
Figure 6:	A Spinning Mass Gyroscope	17
Figure 7:	Ring Laser Gyro	18
Figure 8:	Diagram Explaining Coriolis Effect	19
Figure 9:	MEMs Gyro and the coriolis effect.....	19
Figure 11:	Potential System Block Diagram.....	23
Figure 12:	System Interconnect Diagram.....	26
Figure 13:	IMU Prototype.....	27
Figure 14:	ADXL203 2-Axis Accelerometer Schematic	29
Figure 15:	ADSL203 Evaluation Board Layout	30
Figure 16:	ADXRS150 Gyro Schematic.....	32
Figure 17:	ADXRS150 Evaluation Board Layout	33
Figure 18:	Software Flowchart.....	36
Figure 19:	Software Validation - Movement in X and Y Axes - No Rotation	40
Figure 20:	Software Validation - Rotation and Movement in Y Direction.....	41
Figure 21:	Software Validation - Rotation and Movement in X Direction.....	42
Figure 22:	Step 1 - Initial Reference Position.....	43
Figure 23:	Step 2 Rotation of Unit.....	44
Figure 24:	Step 3 - Unit Movement	44
Figure 25:	Step 5 - Calculations.....	44
Figure 26:	Stationary Data in Initial Test.....	47
Figure 27:	Stationary Test with Threshold Filtering.....	48
Figure 28:	Test 3 Y-Axis Acceleration	49
Figure 29:	Gyro Raw Data – Stationary.....	51
Figure 30:	Stationary Test 5 X-axis vs Time	52
Figure 31:	Stationary Test 5 Y-axis vs Time	52
Figure 32:	Stationary Test 5 Gyro Degrees vs Time.....	53

Figure 33: SR50 Series Rotary Stage.....	54
Figure 34: Test 8: 90 Degree Rotation.....	55
Figure 35: Test 5: -90 degree rotation.....	56
Figure 36: Test 5 X-Axis Movement seen by Accelerometer.....	58
Figure 37: Position Seen by Logger Pro Software and Vernier Equipment.....	59
Figure 38: Simultaneous X and Y axes movement.....	60
Figure 39: Unit Movement in 2D Testing.....	61
Figure 40: Square 2D Test Data Points.....	61
Figure 41: Noise Spike Outside Threshold Range.....	63
Figure 42: Bias Calibration.....	64
Figure 43: Final Position with Software Calculated Bias.....	64
Figure 44: Final Position with Averaged Data Set Bias.....	65
Figure 45: 50 point Averaged Test 1 Accelerometr.....	66
Figure 46: 50 Point Averaged Test 2 Accelerometer.....	66
Figure 47: 50 Point Averaged Gyroscope.....	67
Figure 48: Typical Output Variance due to Temperature.....	69
Figure 49: Maximum Output Variance due to Temperature.....	70
Figure 50: Gyro Output v Temperature.....	72

V List of Tables

Table 1: ADXL203 Evaluation Board Capacitor Values.....	30
Table 2: ADXL203 Pin Configuration and Descriptions.....	30
Table 3: ADXRS150 Eval. Board Capacitor Values.....	32
Table 4: ADXRS150 Pin Configuration and Descriptions.....	33
Table 5: Stationary Data Collection Results.....	50
Table 6: Rate Table Output Summary.....	54
Table 7: 1-Dimensional Testing Results.....	57
Table 8: 2-Dimensional Testing Results.....	62
Table 9: Accelerometer 1 Zero G Bias Level.....	68
Table 10: Accelerometer 2 Zero G Bias Level.....	68
Table 11: Accelerometer 1, Sensitivity Test.....	70
Table 12: Accelerometer 2 Sensitivity Test.....	71
Table 13: Gyroscope Sensitivity Testing.....	72
Table 14: Gyroscope Self Test.....	73

1 Introduction

In 2005, there were 1.6 million fires that were reported. Each day, firefighters risk their lives to prevent loss of civilian lives. They go to major fire scenes where they do not know layouts of the buildings. They enter the building only to discover that there is zero visibility due to the great amount of smoke and that they cannot find the way out. This problem results in serious injury or death because the firefighters cannot exit the building for their safety. In 2005, 115 firefighters were killed while on duty¹.

On December 3rd, 1999, there was a terrible fire at the Worcester Cold Storage Warehouse. Forty firefighters went to the scene to put out the fire and a few of them went inside to search for a homeless couple. Two firefighters sent out a distress call because they were lost in the warehouse due to the heavy black smoke. Two sets of two-person rescue teams went into the burning warehouse to search for their crew and they, too, became lost. 12 hours passed before the blaze could be controlled. All six firefighters lost their lives that day because it was impossible for them to find an exit. When their bodies were found, each of them was within 100 feet of an exit. After this tragic event, 30,000 firefighters from around the world walked in a procession for the brave men who lost their lives in the terrible fire. This event sparked the minds of many people into developing a better way to locate lost firefighters. In 2003, the National Institute of Justice Office of Science and Technology granted \$1 Million towards development of a system. Professors at WPI teamed up with a common goal – to develop a personnel locator device to prevent any future disasters.

2 Problem Statement

Precision personnel location in an outdoor environment can be achieved with current technologies at a low cost and with high accuracy. In an indoor environment positioning becomes a much more cumbersome task. Present research has explored multiple means of providing precision indoor positioning, but it requires a pre-installed system for each building. Currently, low cost systems that do not require pre-installation have been researched and developed but they are not able to provide the accuracy needed for such a task. This project investigated a possible solution by integrating low cost sensors with intricate software algorithms to characterize the sensors for a positioning system. In our study, we aimed to determine if an accurate, low cost inertial measurement unit can be developed with low cost sensors.

3 Project Goals and Requirements

The goal of this project was to characterize the current performance of MEMs (MicroElectroMechanical system) technology in gyroscopes and accelerometers. This included observing and calculating the degree of accuracy of the outputs that these sensors produce and if filtering algorithms can compensate for the errors seen by these sensors. In completion of this goal, the types of improvements needed for MEMs technology to be reliable enough to be used in inertial navigation systems were determined.

The prototype for this project does not have to be pre-installed. The test bed must have an easy setup and straightforward means to run tests. The system will perform in a two dimensional field. After all the data is collected, the final position will be displayed in a HyperTerminal window. Since the technology of MEMs gyroscopes and accelerometers is changing rapidly and new sensors continue to be designed and produced, the device will be non specific to the type of sensors that are connected.

Testing of the system will provide data and allow the team to characterize the current performance of MEMs technology. This project will allow the team to determine what types of improvements in the technology are needed before it can be used in a personnel location device. In the end this project will determine whether or not a two-

dimensional location unit can be utilized for positioning while obtaining a certain degree of accuracy using low cost sensors.

4 Technical Background

In technology, there are multiple means in which to accomplish a single task. There are a variety of methods used to find positioning when navigating, these include: Global Positioning Systems (GPS), inertial navigation means, Radio Frequency Identification, Direction finding and dead reckoning. Impulse Ultra Wideband can be used as a method for transferring positioning data due to its desirable characteristics.

4.1 GPS

GPS is the most commonly utilized navigation system today with millions of clients². Currently there are two GPS systems in place, the US system of NAVSTAR (Navigation Signal Timing and Ranging) and the Russian system named GLONASS (Global Navigation Satellite System). The European Union is currently developing a system of their own, Galileo. The US system consists of 24 satellites (with 4 additional spares) in a total of 6 orbits (each with 4 satellites)³. On December 8, 1993 it was declared that GPS would be fully operational and provide “continuous time and three-dimensional position and velocity.” Up until recently, car navigation contained the largest consumer market in GPS with over 10 million clients.⁴ Now GPS chips embedded in cell phones has consumed the market.

GPS works by calculating position (latitude, longitude and altitude) based on the time delay it takes for a signal to be received by a receiver. Using precise atomic clocks, the time it takes for the signal to reach the receiver is calculated. By multiplying the travel time by the speed of light distance can be obtained.

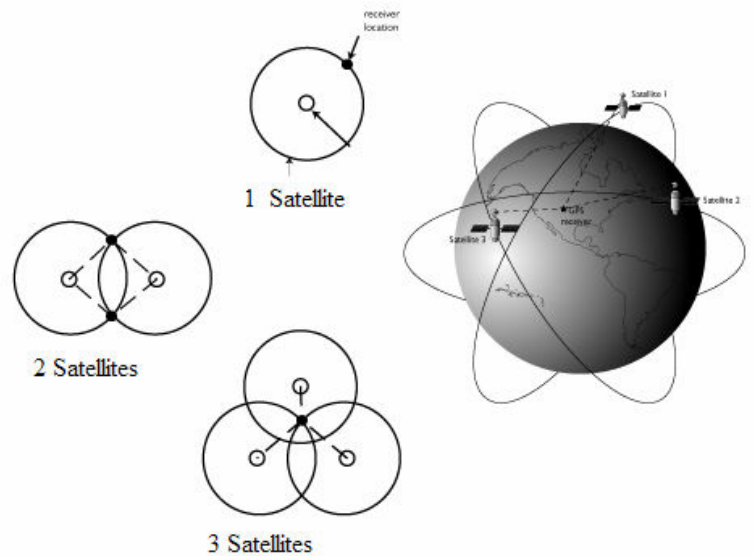


Figure 1: GPS Trilateration Methods⁵

Trilateration methods are utilized to determine accurate location. The point of intersection of the distances from the satellites is how GPS triangulation is accomplished (see Figure 1). The more satellites in range of the receiver the more accurate of a position can be calculated.

Today, GPS is used for the military, personal location based services (in cell phones see Figure 2) and mobile satellite communications such as satellite TV, to just name a few. Present GPS chips can update position as frequently as 40 times a second.⁶



Figure 2: Cell phone using GPS Navigation⁷

Although GPS seems to be a clear cut solution to navigation issues, GPS is lacking when it comes to applications that are non line-of-sight. Satellite signals are not incessantly available everywhere on Earth, especially when indoors. Multipath, when a signal takes two or more paths to reach a receiver, becomes a major problem when trying to obtain an accurate reading. This multipath leads to inaccurate

measurements in time delay, which results in inaccurate distances. Signal attenuation from vegetation is also an issue. One way in which to aid this situation is with a combination of GPS with other navigation methods, such as dead reckoning or other inertial sensors.

4.2 Dead Reckoning

Dead reckoning involves calculating your position by known initial position, speed and direction. As long as you know your speed, course and time you will be able to calculate your positioning. A compass may be used to determine the direction while distance can be calculated by speed and time.

In the 1500s this type of direction finding was common. While on a ship, an object was thrown overboard, also known as a Dutchman's log, and by recording the time it took for the ship to pass by the object (the object was considered "dead" in the sea) the speed of the ship could be determined.⁸

An apparent downfall to the dead reckoning system for navigation is that if there is any change in speed or drift in course, without any means to correct the knowledge, this is no longer an acceptable solution for navigating. With newer technology calculating speed and the direction can be made easy but before such technological advances it was difficult. Relying upon known landmarks, or fixes, a new start of positioning could be established.

4.3 Impulse Ultra-Wide Band

An Ultra-Wideband (UWB) pulse is a pulse that is transmitted across a wide range of frequencies. These signals can be very valuable for navigation systems due to their high precision. Since UWB systems have highly accurate timing, there is a distinct separation between multipath propagation and the actual signal. This is very helpful in buildings where signals can be reflected by objects. With a large bandwidth, there is more resolution which provides better accuracy of the system. The bandwidth of the signal is at least 20% of the center frequency.⁹ For instance, if a signal that is centered at 4 GHz, the bandwidth would be at least 800 MHz.

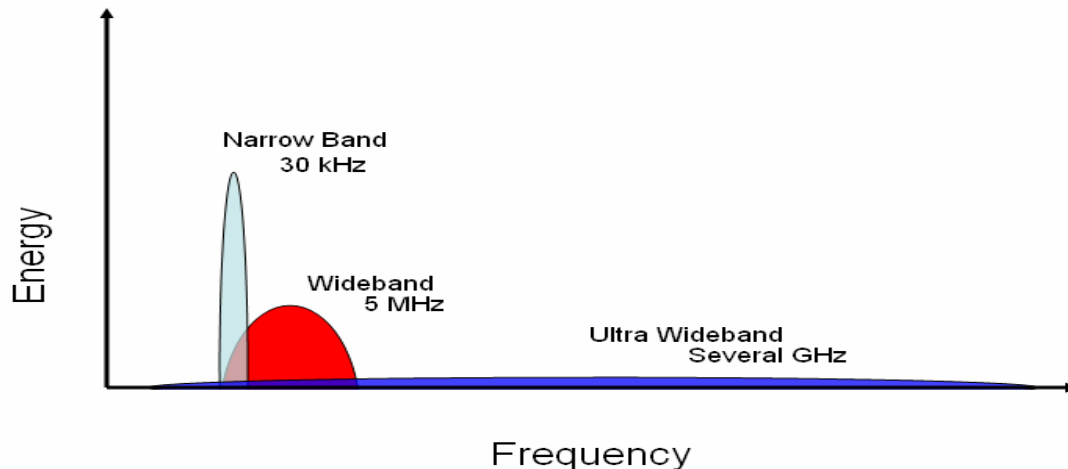


Figure 3 - Bandwidth of Signal Types

Ultra-Wideband signals are very small in duration. They generally range from 50 to 1000 picoseconds for each pulse. Each of these pulses represents one binary state (a logic 0 or 1). The pulse will either have a high amplitude to represent a logic 1 or a low amplitude to represent a logic 0. A transmitter sends out billions of these pulses, which could look like nothing more than noise. A high-speed sampling receiver is required to be able to read these signals. These very short pulses on a direct path arrive to a receiver faster than any multipath signal, which can eliminate multipath error. The receiver deciphers the signal by listening for a repeating pulse sequence that was sent by the transmitter.

The Federal Communications Commission (FCC) allows commercial UWB products to operate between 3.1 to 10.6 GHz.¹⁰ They believe that these signals could interfere with other transmissions. However, due to the wide frequency spectrum, low power, and very short signal pulses, these systems do not interfere with other transmissions nearly as much as narrowband signals. Also due to the characteristics of UWB, the signals are also resistant to other electrical interference with other wireless devices.

This technology has caught the eye of many electronics companies due to several benefits over the narrowband. Since the signals are being transmitted over a wide spectrum of frequencies, there is a lot of information sent out in each pulse. This can allow for data to be sent at a very fast speed (hundreds of gigabits per second).¹¹ Since

UWB signal is distributed over several gigahertz, the spectral density is very low. The FCC limited the power of the signal that can be transmitted to 75 nanowatts of power per megahertz of frequency bandwidth.¹² With this limitation of power, UWB signals have very low power requirements. This also leads to a limited range of transmission.

4.4 Direction Finding

A direction finding device works by pointing a directional antenna in different directions to determine where the strongest signal is coming from. Originally, direction finding was used in World War II. Airplanes were looking for boats that were transmitting messages. Antennas were attached to the airplanes during the war to locate the direction of the signal. Once they knew the direction of the transmitter, the planes would target the boats.



Figure 4: Solenoid¹³ and Directional Antenna¹⁴

Currently, solenoids are being used instead of a directional antenna. A solenoid is made up of coils of wire. For the solenoid to be used in direction finding, it would be spun around on a motor. The solenoid is used as an antenna to pick up signals. The system would monitor the incoming signals through the solenoid for reoccurring peaks in the signal. The opposite approach is to listen for spots where the signal is repeatedly at 0. This occurs when the antenna is orthogonal to the signal. When the signal is orthogonal to the antenna, the antenna cannot receive the signal from the transmitter. The transmitter is then known to be in one of the two directions orthogonal to the antenna when the signal is 0.

Homing devices rely on signal strength to determine direction and location of a signal. The basic concept of homing devices is that the signal becomes stronger when the receiver is getting closer to the transmitter. As the signal gets stronger, a direction of the transmitter is established. A previous Major Qualifying Project (MQP) was a device called the “Man-Tenna” is a directional RF homing device that uses frequencies between 160 and 190 KHz. At these frequencies, it can penetrate metal sheets that can be in walls. The current version of the device has a range of 50 feet.

4.5 Inertial Navigation

Inertial Navigation is, “A self-contained system which can automatically determine the position, velocity, and attitude of a moving vehicle for the purpose of directing its future course”.¹⁵ The basic element in determining position in an inertial navigation system is acceleration. In order to determine the acceleration in all axes, three accelerometers placed orthogonally on the X, Y and Z axes (according to Figure 5) are necessary. The orientation of the axes is crucial for accurate calculations. In order to initialize the inertial sensors, a known orientation must be specified by the user. Once the system is in motion, recalibration is needed to ensure the accurate orientation of the axis. Some systems are recalibrated every few seconds while others do not need to be recalibrated for weeks or months. This will vary from application to application. Motion in any of the directions will be detected and then velocity and ultimately position can be determined. The following equations are used to determine velocity, displacement and angular rotation:

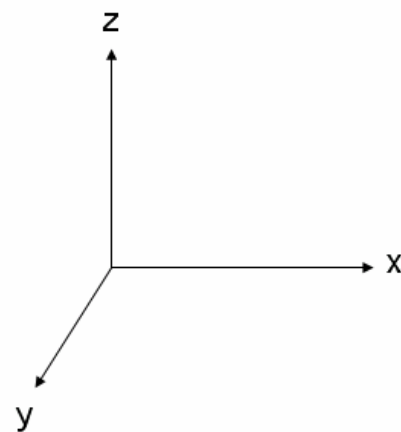


Figure 5: Three dimensional axis

$A(t)$ $V(t) = v_0 + \int_{t_1}^{t_2} a \, dt'$ $P(t) = p_0 + \int_{t_1}^{t_2} v \, dt'$ $R(t) = r_0 + \int_{t_1}^{t_2} b \, dt'$	$A(t)$ = Acceleration from accelerometer $V(t)$ = Current velocity V_0 = Previous velocity $P(t)$ = Current displacement P_0 = Previous displacement $R(t)$ = Current rotation in degrees R_0 = previous rotation in degrees
---	--

Inertial navigation systems have been developing since the Second World War.¹⁶ They consisted of accelerometers and mechanical gyroscopes. The gyroscopes were not very reliable and required a lot of power. Today, new technologies allow for solid state solutions for these systems.

Inertial navigation systems are made up of multiple sensors. These typically include a combination of accelerometers, to measure the acceleration of an object; gyroscopes, to measure the angles of rotation; and compasses and magnetometers to find true north to aid in calibrating the system. Inertial navigation systems are used in a wide variety of applications. They can be used for location of civilian and military planes, or guiding missiles. For some of these applications, accuracy and reliability are major factors. To make inertial navigation systems as precise and reliable as possible, expensive components must be used. As a result, the cost of the systems drastically increases. They can cost anywhere from hundreds of thousands of dollars to millions of dollars.

4.5.1 Accelerometers

Micro-Electro-Mechanical System (MEMS) accelerometers are common in today's world. There are different accelerometers that can measure acceleration in one, two, or three axes. High G accelerometers measure +/- 20 to 250 G, while low G accelerometers measure +/- 1.7 to 10 G. There are multiple applications that they can be used in, including measuring position, motion, tilt, shock, and vibration. As the name suggests this technology merges both electrical and mechanical components. In capacitive sensing accelerometers, the capacitance correlates to acceleration. There are both fixed plates and plates attached to polysilicon springs. When a force is applied, the

plates attached to springs shift and change the distance between them. This in essence changes the capacitance which is proportional to the applied acceleration.

MEMS accelerometers have become fairly inexpensive over the years. Analog Devices manufactures MEMS accelerometers that range from \$7 to \$28.¹⁷ Over the past few years, accelerometers have become easier to use, more functional and more reliable. Many accelerometers now have the capability of sensing linear acceleration in 3 dimensions (X, Y, and z axis).

MEMS accelerometers require input voltages of a minimum of 3 volts to a maximum of 6 volts, with a quiescent supply current from 0.5 to 0.7 mA. The temperature ranges from -40 to +125 degrees Celsius. For low-g accelerometers, ranges of ± 1.2 g to ± 18 g are typical. High-g accelerometers have much greater ranges from ± 35 g to ± 250 g. With a low-g accelerometer greater sensitivities to smaller accelerations can be obtained allowing for a higher resolution of its output voltages. The low-g allows 1000 mV per g sensitivity while the high-g only allows 8 mV per g. The resolution of the low-g accelerometer is much greater because it only needs to represent ± 1.2 g to ± 18 g over 5 volts. The high-g accelerometers must also represent their range over 5 volts, leading to a lower resolution.

A higher measurement resolution will allow for smaller detectable acceleration. The bandwidth of these sensors range from 0.5 Hz to 2.5 kHz. External capacitors must be used to set the bandwidth. The combination of the external capacitors and the internal resistors create low-pass filters that limit the bandwidth to provide noise reduction and anti-aliasing.

Many companies focus on power consumption of accelerometers. Most accelerometers consume less than 1mA of power. There are available options that focus on obtaining better battery life. For example, there is a power down mode where the accelerometer powers down and consumes much less current (around 10 μ A) and will power on when it is interrupted with a quick change in acceleration.

4.5.2 Gyroscopes

A Gyro is “A device that is used to define a fixed direction in space or to determine the change in angle or the angular rate of its carrying vehicle with respect to a

reference frame.”¹⁸ A gyro measures the rate of change in angles between axes. Among other things gyros are used for navigation, guidance and stabilization.¹⁹ Examples of these are: to measure the deviation of a guided missile; to measure the bearing of a car; and to determine the bearing of a craft for direction-finding.

One important aspect of the gyro is that its performance is measured in drift-rate per unit time, also known as degrees per hour.²¹

For example, if the gyroscope on a ship sailing on the sea at the equator is experiencing a drift rate of $0.0167^\circ/\text{hr}$, a corresponding distance can be evaluated from the definitions stated below:

$$1 \text{ minute of arc} = 0.0167^\circ$$

$$1 \text{ minute of arc} = 1 \text{ Nautical mile}$$

$$\text{Therefore: } 0.0167^\circ = 1 \text{ Nautical mile}$$

Since the gyro is experiencing 0.0167° of drift per hour, that corresponds to a drift of 1 Nautical mile per hour. After one hour the calculated displacement will be off by 1 Nautical mile from the actual displacement.

Other errors include bias, temperature, and acceleration. Temperature effects can cause error such as thermal drift. Other sources of error include bias, this occurs when the gyro has an output reading when there is no input. Such errors can be compensated in the navigation computer to some extent, but residual errors may remain.

There are multiple types of gyroscopes available. A spinning mass gyro (see Figure 6) isolates the spinning mass in a case so that it may remain fixed in space. The position of the mass to the case is relative to the angle of rotation.

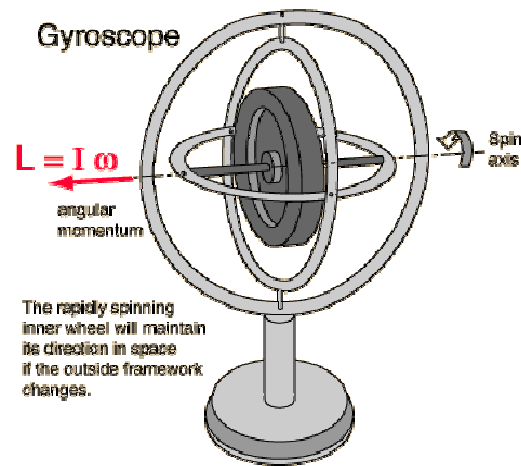


Figure 6: A Spinning Mass Gyroscope²⁰

The ring laser gyro (RLG), invented in the 1960s is actively used in navigation and tactical systems.²³ A laser beam is split and then directed into two opposite directions around a closed path. The time difference in which it takes both of the beams to travel around the path and be detected by the detector is proportional to the speed of rotation that the gyro is experiencing. Most RLGs are square or triangular shaped. Mirrors placed at each corner reflect the laser around the loop.

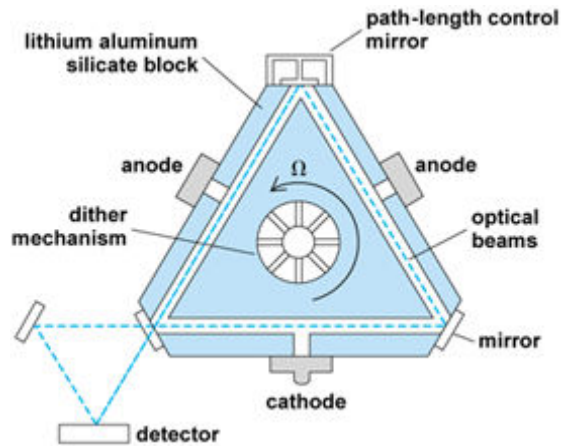


Figure 7: Ring Laser Gyro²²

A disadvantage of the RLG is that if little movement is detected and the frequencies of the moving beams do not have a large differential then it is possible for the gyro to have a zero rotational reading, this is called lock in. RLG technology was originally explored for use for strapdown applications because it has exceptional stability and linearity and has insignificant sensitivity to acceleration.²⁴ They are literally “strapped” down to an object such as a car and measure the car’s angular rate changes. Another platform in which gyros are placed is called a gimbaled platform. On a gimbaled platform the gyroscope keeps its orientation while the vehicle rotates around it. A major disadvantage for using this type of platform is cost of the precise mechanical parts, that over time will wear and could lock the system in place.

For some applications, MEMs gyros are equivalently meeting the performance of other gyros. They are now smaller in size and cost and can obtain the similar performance characteristics.²⁵ MEMs technology is very often found in automobiles to measure tilt and skid for better handling and control.²⁶ These types of gyros measure angular rates by using the Coriolis effect. The Coriolis effect takes into account the change in position of the final destination due to rotation. For instance when an object moves in a straight path on a rotating platform the Coriolis effect is experienced (Figure 8). Although an object is moving in a linear fashion, it has an increasing angular velocity as it nears the edge of the platform. This velocity in combination with the velocity at which the object is moving is the Coriolis effect. This phenomenon happens in airplanes,

when traveling from one point to the next. If the Coriolis effect was not accounted for the airplane would miss its final destination.

The Coriolis force equation is shown below:

$$F = 2Mv * \Omega$$

Where:

F = force

M = Mass

v = velocity (of the moving object)

Ω = angular velocity

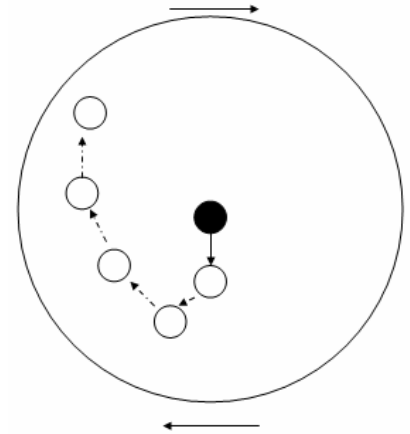


Figure 8: Diagram Explaining Coriolis Effect

For instance an object placed near the center of a rotating circle has a lower angular velocity than an object placed at the outer edge of the circle. Figure 9 shows the

mechanical structure of this type of gyro. A resonating mass is attached to the inner frame by springs. As the gyro experiences motion about the axis which is perpendicular to the top surface of the gyro the “coriolis sense fingers” measure the displacement of the mass by a change in capacitance produced by the force of the mass in a given direction.²⁸

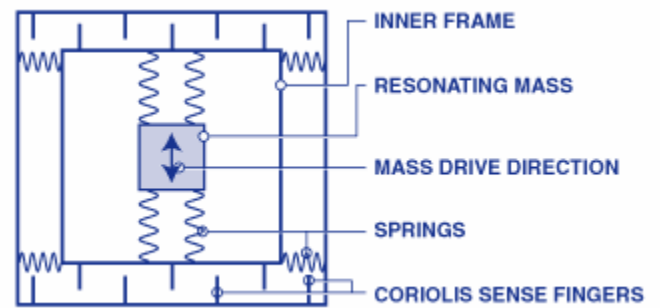


Figure 9: MEMS Gyro and the coriolis effect²⁷

Figure 9 shows the axis of rotation of a MEMS gyro that produces a positive output voltage when experiencing clockwise rotation.

Analog Devices produces MEMS gyros starting at \$30. These gyros are single axis and have a rotation range of up to ± 300 %/sec. A temperature sensor is already built internally to the device. This temperature reading can be incorporated into a thermal drift compensating algorithm to reduce the thermal noise of the sensor. Analog Devices also manufactures 2 and 3 axis gyros, some with self-test modes that double check the device is functioning.

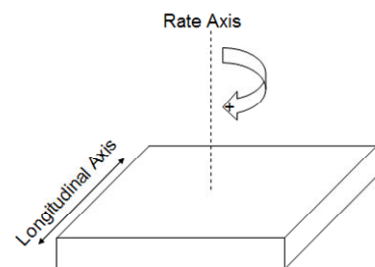


Figure 10: View of Gyro and axis of rotation

MEMS gyros require an input voltage of a minimum of 4.75 volts to a maximum of 5.25 volts, with a quiescent supply current from 6 to 8 mA. The operating temperature

ranges from -40 to +85 degrees Celsius. Rotation range for these gyros are anywhere from ± 75 °/sec to ± 300 °/sec, with a sensitivity of $15 \pm 15\%$ to $5 \pm 8\%$ mV/°/sec. The bandwidth of these sensors is DC to 2000 Hz with a noise density ranging from 0.05 to 0.1 °/sec/ $\sqrt{\text{Hz}}$. External capacitors can be used to set the bandwidth, this is important when trying to achieve the best bandwidth with some noise trade offs. This can be accomplished because the combination of the external caps and the internal resistors create low-pass filters the limit the bandwidth. A majority of these gyros have shock ratings of up to 2000 g³⁰.

It is important when choosing a gyro to understand the rotary rate of each sensor. The question to ask would be “How fast can the gyro turn and still output an accurate signal?” The outputs of the gyro come in many forms, either through voltage, current or frequency. In a gyro that produces a voltage output for instance, each voltage corresponds to a particular angular rate. As the gyro is rotated the output voltage will fluctuate proportionally to the angular rate at which it is turned. The outputs of gyros work much like the outputs of the accelerometers.

4.5.3 Sensor Error

There are various sources of error that heavily impact the performance of these MEMs sensors. These are both internal and external aspects that influence implementation. These errors include drift, nonlinearity, misalignment, noise, temperature variation and computational errors. Through extensive research and testing it is possible for computational models to be developed for some sources of error that could be compensated for. Then perhaps MEMs devices could be the sole components used in a navigation device. However these models would be extremely complex and require an indeterminate amount of time and expensive equipment.

Drift occurs in both the accelerometer and the gyroscope. Drift is a gradual error that inevitably makes output readings and calculations inaccurate. Drift occurs when the output shows a change in time with a stable input. Drift can be due to a changing sensitivity or offset that may or may not relate to a change in temperature, pressure or light³¹. With continual re-calibration drift errors can be diminished.

Thermal drift is a concern with MEMS devices. Output specifications vary depending on the temperature, not only ambient temperature but more importantly the temperature of the device. The specification sheet for the accelerometer states that thermal drift compensation is built into the sensor, therefore temperature drift is extremely low, ranging around 10mg over the entire operating range. However external temperature sensors could be used in conjunction with the accelerometer to keep track of the operating temperatures. With understanding how the accelerometer output changes due to a change in temperature, the output can be compensated using a software model. The gyroscope used in this application has a built in temperature sensor that can be read like all the other outputs. The sensor outputs a voltage that is proportional to temperature, for 27°C 2.5v is seen on the output. Using some advanced calibration techniques this temperature drift can be compensated for like the accelerometer. It is possible to use the temperature output of the gyro as basis for the accelerometer, therefore eliminating the need for an additional temperature sensor. Further research shows that temperature drift does reach a steady state between 2 and 12 hours. One way to reach this steady state earlier would be to increase the temperature of the sensors to its normal operating temperature shortly after start-up therefore allowing some linear assumptions to be made.

There are two types of alignment errors, Sensor-level and System-level errors. Sensor level errors occur when there is error between the orthogonal axes. For instance in the dual axis accelerometer, although much caution is taken during the fabrication process to ensure the two axes are exactly 90 degrees apart, there could be some deviation leading to some inaccurate output readings. System level errors result in mounting errors of the sensors. There could be some machining factors so the surface is not flat, or the PCB has some irregular fluctuations in the board. If the misalignment can be calculated or measured it is possible that this error can be calibrated for. Current systems being developed use Kalman filtering to aid in this inaccuracy.

Much of the noise output by the sensors is white-Gaussian noise and power supply noise. The noise from the power supply can be decoupled simply with the use of a capacitor, making this source of error the most straightforward and simple noise to deal with. Gaussian noise is more complex, limiting the bandwidth may help but simple

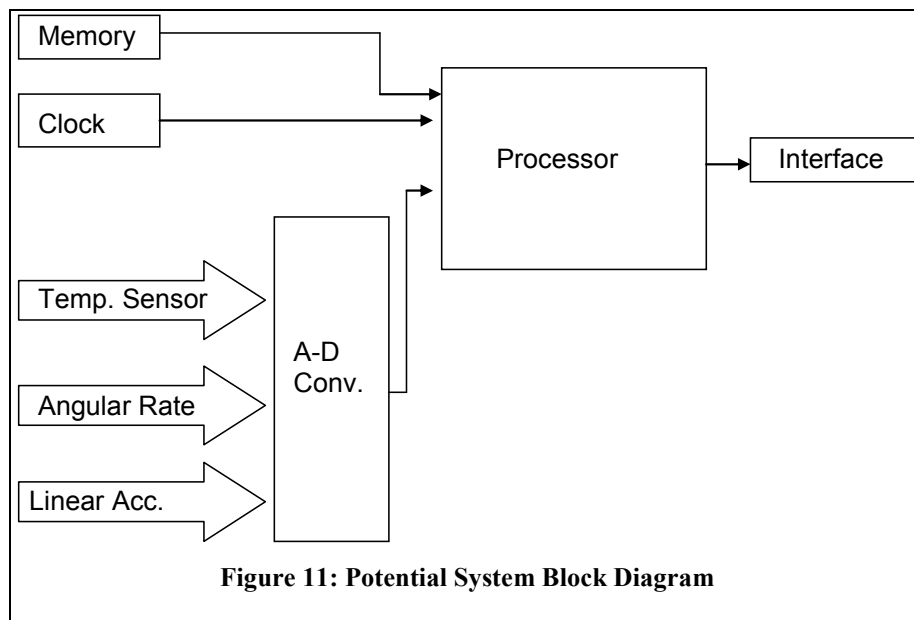
filtering or extremely complex filtering such as Kalman filtering can be employed to reduce this noise further.

A small variation in output voltage could result in a large position error. This is due to the fact that each accelerometer output is integrated twice to find the distance, hence the error is also integrated. Computational errors also arise when formulas or decimals are truncated due to coding and memory size. An additional computational error occurs when a small error in the system is integrated to find velocity and then position.

4.5.4 Magnetometers and Compasses

A magnetometer is a device used to measure the strength of a magnetic field. There are two types of magnetometers, scalar and vector. A scalar magnetometer measures the overall magnetic field around it while a vector magnetometer is able to measure the component of the fields in a specific direction. A magnetometer can be used to ensure proper location of the earth's Magnetic North as well as to ensure the gyroscopes are obtaining accurate measurements. True North is the direction of a longitudinal meridian that converges at the North Pole. Magnetic North is the direction given by a magnetic compass. The difference between these two poles is called magnetic declination, which is the angle of difference between the end of a compass and True North. Magnetic declination varies from place to place and in time. A magnetometer in conjunction with a compass would allow the user to obtain an accurate heading, by understanding where True North is.

4.6 Potential System Block Diagram



The initial system block diagram consisted of the sensors going into analog to digital converters, then fed into the processor to perform the calculations and then output the results. The processor would have memory to store the data taken in by the sensors and a clock for timing.

4.7 Processing Unit

There are several different types of microprocessors in the market at the moment. Companies such as Microchip and Texas Instruments produce a wide variety of microcontrollers. A microcontroller is a type of microprocessor that is self-sufficient, where almost everything that is needed to run (i.e. memory and interfaces, etc) is already built in. A general microprocessor requires additional chips to run. The microprocessor that would best fit this system needs to be powerful enough to perform many algorithms on the input signal. Some implied specifications of the microprocessor are ease of use, at least four inputs to receive the data from the A/D converter (two accelerometers and two gyroscopes), and small in size.

Microchip produces many different lines of microprocessors, called PIC Microcontrollers that are either 8-bit or 16-bit. The PICs use assembly as the coding language. The memory in the microcontroller can range from .5 KB to 256 KB and are of different types. There are flash, one time programming, and read only memory. The microcontrollers have speeds from 4 MHz to 64 MHz.

The main programming language that is being used to program the PIC is assembly. However, with newer technology and different compilers, the C programming language can be used instead of assembly. Both languages are able to fully utilize the microprocessor.

These microcontrollers are capable of many different applications like interfacing universal serial bus (USB), communication through Ethernet or RF transmissions, to displaying on Liquid Crystal Displays (LCDs).

A company called Gumstix designed very small motherboards that can run Linux. By running Linux on the processor, C, C++, Java, Perl, or Python programming languages can be used to do any processing.

These processors can run from 200 MHz to 400 MHz, depending on which motherboard is selected. They are around the size of a stick of gum (20mm X 80mm X 8mm).³² An option for the motherboard is to have a 62-pin connector and/or a 92-pin connector, which allows for expansion boards to be attached for additional functionality. To communicate with a Gumstix processor, a serial or Ethernet connection can be used. Some boards that can be used for expansion are 802.11b/g wireless, 10/100 Ethernet, secure digital or compact flash readers, analog audio, USB, Analog-to-Digital Converters, or serial ports.

4.8 Memory Storage

Two essential characteristics when determining what type of memory to choose for the system are that it is high density and it is non-volatile. High density will ensure that all of the raw data collected during a trial can be stored, without the memory storage becoming completely full. A non-volatile system is extremely important in case of battery loss. This will guarantee that all of the information will be saved without fear of losing it in case power is no longer applied. There are multiple types of memory

available on the market. This includes: removable USB, Compact Flash, and Secure Digital (SD) cards to name a few.

Removable USB is a type of flash drive with a USB interface that comes in sizes of 60 MB to 8 GB. Due to the lack of moving parts in such a device (solid state), it is considered to be more reliable than the once so popular floppy disk. Internally, this device is made up of a printed circuit board which is encased in a durable plastic for protection (it can be carried around in a pocket without much care). These devices are powered by the source in which they are connected to such as a computer. USB 2.0 allows raw data rates of 480 Mbps (this is much faster than the 12Mbps of the prior USB 1.1). Typical applications of for USB include transportation of personal files including music, pictures and documents; carry around an application that may be run off the drive; and it can contain recovered programs to repair a computer in case of infection.

Compact Flash (CF) is most popular in portable devices. It uses non-volatile Flash memory (blocks of data that can be erased and reprogrammed) to save and store information. CF comes in typical storage sizes ranging from 2 MB to 4 GB, with write speeds up to 6 Mbps³³. Common applications include digital cameras, cell phones and pagers.³⁴

Secure Digital memory is also a non-volatile, solid-state, flash drive. Storage sizes range from 128 MB to 2 GB. Data transfer rates (read and write) for this device are approximately 6 -10 Mbps, although high speed SD is available at 15 Mbps. Applications for this memory type include GPS receivers, digital cameras, cell phones and PDAs. Of the three memory types discussed here, SD is the smallest in size, approximately the size of a postage stamp.

5 Final Design

After reviewing the major components required for the unit a final design was put into place. A review of the entire system and its capabilities is provided, then followed by a detailed breakdown of each component. This unit is an integration of both hardware and software that intricately work together to provide an inertial measurement unit.

5.1 Physical Parameters

The system consists physically of the processing unit, protoboard, and battery pack. In the processing unit, there is the Gumstix processor, compact flash card reader, Robostix (A/D converter), serial connector, AC adapter, and notification LEDs. The Gumstix processor is used to process the data. It is a 200 MHz microprocessor that runs the Linux version 2.6 operating system. It has a 62-pin connector or a 92-pin connector, which allows expansion boards to be attached for additional functionality. To communicate with a Gumstix processor, we use the serial port. HyperTerminal in Windows is used to display the outputs on the Gumstix.

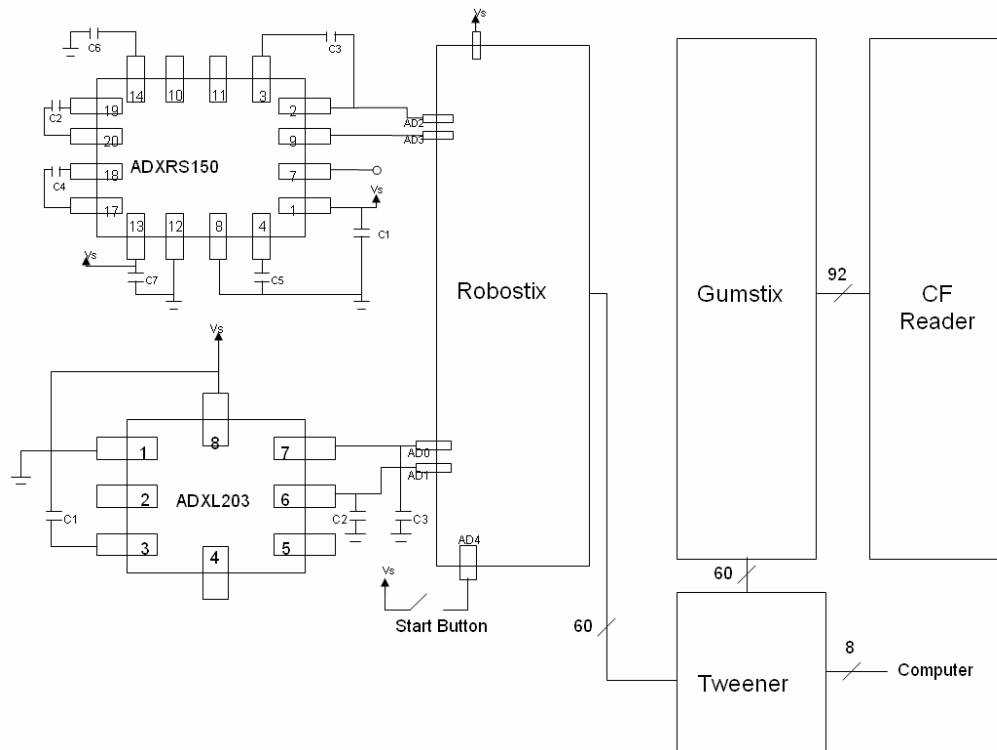


Figure 12: System Interconnect Diagram

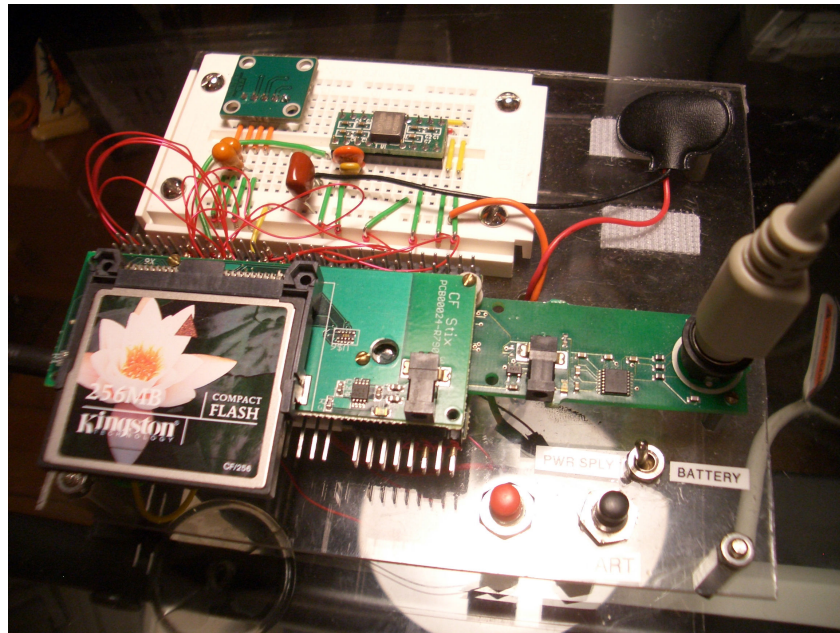


Figure 13: IMU Prototype

The expansion boards that are used are the Compact Flash board, tweener, and Robostix. The compact flash (CF) board is used as the non-volatile memory for the device. The tweener gives us an interface to a computer to control the Gumstix. The Robostix contains the analog-to-digital converters that are needed to take in the data from the accelerometer and gyroscope.

The notification LEDs are helpful when the system is not connected to a computer to see what step the unit is currently in. The red LED states that the Gumstix is communicating to the Robostix. When the blue LED is on, the system is calibrating the gyroscope. A blinking yellow LED signifies that it is calibrating the accelerometers. The blinking blue LED means that the system is gathering data.

The protoboard has a 2-axis accelerometer and gyroscope on it. There is also a start button to tell the unit when to begin gathering data from the sensors. There is a switch to turn the battery pack on and off that is attached to the plexiglass.

The prototypes is non-sensor specific. Assuming the same output format (analog) and 5 volt input voltage, any sensor can be placed on the protoboard for evaluation. This is useful when wanting to characterize new sensors performance.

5.1.1 Sensors

The sensors were ordered on evaluation boards due to difficult packaging, the accelerometer being leadless and the gyro being ball grid array. This also allowed for faster evaluation of sensor outputs by eliminating the need for additional circuit assembly. The evaluation boards were packaged such that prototyping on a breadboard was made easy. Each sensor also has a self-test such that when 5 volts is applied an output of 2.5 volts on the self test pin proves the sensor is properly functioning. An explanation of each of evaluation boards is included below.

5.1.1.1 2-axis Accelerometer ADXL203

The ADXL203 accelerometer used in this project is a “high precision, low power, complete dual-axis accelerometer with signal conditioned voltage outputs, all on a single, monolithic IC”³⁵. This sensor is a polysilicon surface-micromachined structure that is constructed on top of a silicon wafer. Polysilicon springs hold the structure over the wafer and supply a resistance against any acceleration force. Any deviation of the structure is measured with a differential capacitor. This type of capacitive sensing accelerometer is known for its higher accuracy, stability, and low noise compared to other sensing types. However, due to the high impedance of the sensing nodes, proper packaging must be attended to in order to eliminate the effects of electromagnetic interference.

Figure 14 shows the full schematic of the two-axis accelerometer evaluation board connected to the Robostix. The ADXL203 has a full scale range of $\pm 1.7G$ measuring dual-axes. The board contains a five pin header for easy access to power, ground and the output signals. Figure 15 shows the layout of the evaluation board including the sensor, header pins, and capacitors.

This sensor requires 3v to 5v to operate. It must be kept in mind that this sensor is ratiometric, meaning the output sensitivity is proportional to the voltage supply. At $V_s = 5v$ the output has a zero G DC bias of 2.5v, if the supply voltage varies so does the output bias and must be compensated for when completing calibration and any additional calculations. The ratio of these voltages is as follows:

$$V_o (0G \text{ DC Bias}) = .5 * V_s$$

This accelerometer is able to measure both positive and negative accelerations in both axes. A positive acceleration is known when V_{out} is greater than the 0G DC bias while a negative acceleration is known when V_{out} is less than the 0G DC bias. For instance, if the accelerometer is operating at 5 volts our bias is at 2.5v, then for any output greater than 2.5v is positive acceleration, any output less than 2.5v is negative acceleration and any output equal to 2.5v is not accelerating.

Capacitor C1 in the schematic is used to decouple the power supply. A 0.1uF capacitor is used in many applications in order to decouple the noise from the power supply, thus $C1 = 0.1\mu F$. Capacitors C2 and C3 are used to set the bandwidth. These are needed in order to create a low pass filter that will prevent aliasing and reduce noise. The bandwidth of this accelerometer can range from 0.5 Hz to 2.5 kHz; it can be adjusted by the user for appropriate bandwidth settings. The evaluation board sets C2 and C3 to 100nF which sets the bandwidth to 50 Hz. This bandwidth may be adjusted by adding additional capacitors to the circuitry. There is a bandwidth versus noise tradeoff however, the higher the bandwidth the higher noise³⁶.

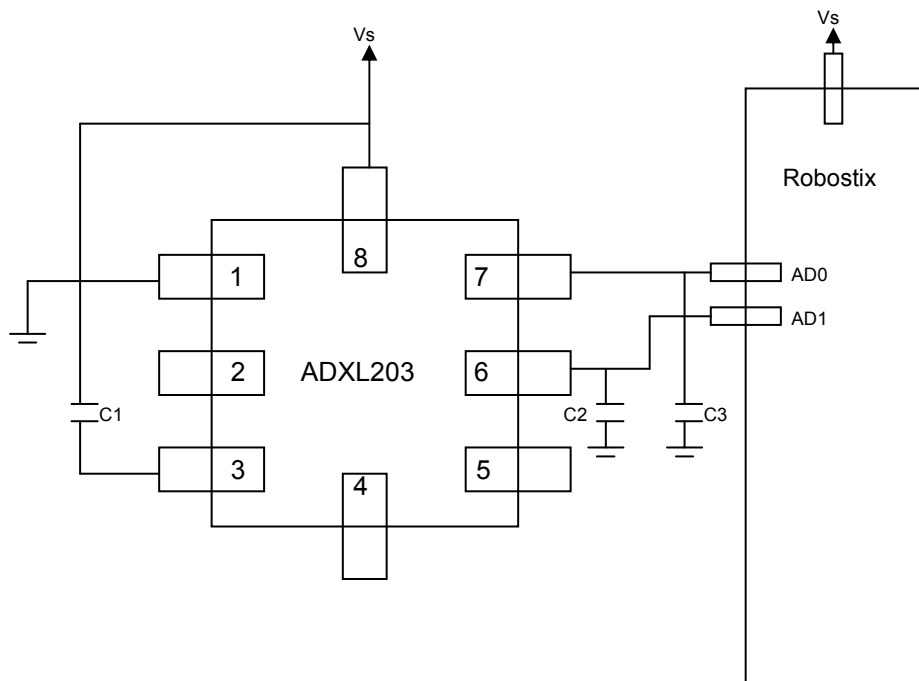


Figure 14: ADXL203 2-Axis Accelerometer Schematic

Capacitor	Value (uF)
C1	.1
C2	.1
C3	.1

Table 1: ADXL203 Evaluation Board Capacitor Values

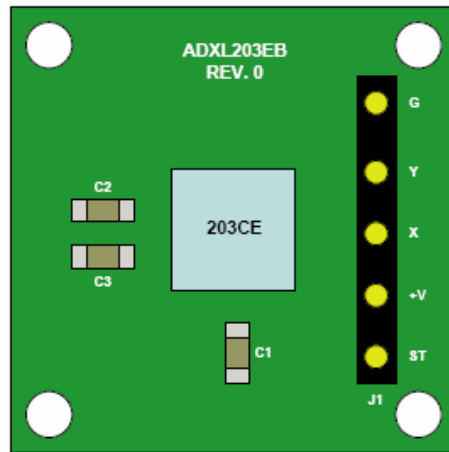


Figure 15: ADSL203 Evaluation Board Layout³⁷

Pin	Explanation
1 - ST	Self Test
2 – DNC	Do Not Connect
3 – COM	Common
4 – DNC	Do Not Connect
5 - DNC	Do Not Connect
6 - Yout	Y Channel Output
7 - Xout	X Channel Output
8 - Vs	3v – 6v

Table 2: ADXL203 Pin Configuration and Descriptions

5.1.1.2 Yaw Rate Sensor Gyroscope ADXRS150

The ADXRS150 evaluation board was obtained from Professor Furlong as a free sample, making our decision on which gyro to use a simple one. The board is a 20-pin dip package that once again allows for easy prototyping on a breadboard. Figure 16 shows the full schematic of the gyro connected to the Robostix, while Figure 17 shows the evaluation board layout.

This angular rate sensor requires 4.75v to 5.25v to operate. Unlike the accelerometer its output is not ratiometric. However it has a null reference of 2.5v of which to base clockwise and counterclockwise movements from. The output signal is proportional to the rotation rate around the axis normal (z axis) to the top plane of the sensor. A rotation in the clockwise direction will result in an output voltage greater than 2.5v while any angular rotation in a counter clockwise direction will result in an output voltage less than 2.5 volts. In order to ensure the null voltage is 2.5v which we base all of our additional calculations from calibration software is provided.

Due to the nature of operation of this gyro, charge pump capacitors are needed in order to create a 14v – 16v supply, due to the fact that only 5v are required to power the sensor. This charge pump powers an electrostatic resonator that will produce the needed coriolis effect for a properly functioning gyro. Capacitors C2 and C4 each with 22nF values are used to create the charge pump. C1, C5, C6 and C7 are all decoupling capacitors. C3 is a 22nF capacitor used to set the bandwidth to 40Hz. Like the accelerometer this bandwidth can also be adjusted according to user specifications. Table 3 **Error! Reference source not found.** lists the capacitor values that come standard on the evaluation board³⁸.

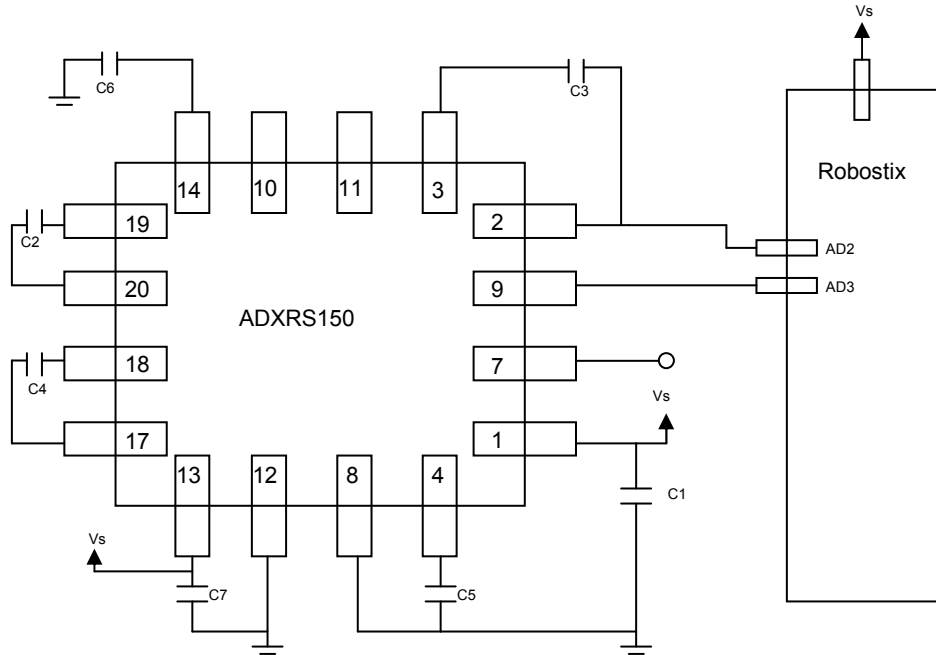


Figure 16: ADXRS150 Gyro Schematic

Capacitor	Value (nF)
C1	100
C2	22
C3	22
C4	22
C5	100
C6	47
C7	100

Table 3: ADXRS150 Eval. Board Capacitor Values

Pin	Explanation
1 - AVCC	+ Analog Supply
2 – Rate Out	Rate Signal Out
3 – SUMJ	Output Amp Summing Junction
4 - CMID	HF Filter Cap 100nF
7 – 2.5V	2.5v Reference
8 - AGND	Analog Supply Return
9 - TEMP	Temp. Voltage Output
10 – ST2	Self Test Sensor 2
11 – ST1	Self Test Sensor 1
12 - PGND	Charge Pump Supply Return
13 - PDD	+ Charge Pump Supply
14 – CP5	HV Filter Cap 47nF
17-20 CP4 – CP1	Charge Pump Filter Capacitors

Table 4: ADXRS150 Pin Configuration and Descriptions

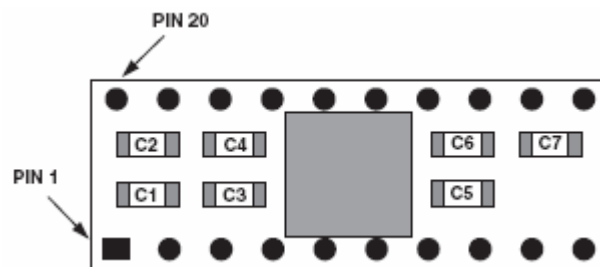


Figure 17: ADXRS150 Evaluation Board Layout³⁹

5.1.2 Processor

Gumstix has processing packages available that include several different expansion boards. The Robostix CF (compact flash) pack was chosen to be the processing unit. It includes the processor board (Gumstix), an eight input expansion board with analog to digital converters (Robostix), compact flash interface board, and a serial interface board to communicate with a host computer. This package includes all of

the hardware needed to build the system, minus the sensors. This is a convenient solution for the needs of the design.

The processor contains a 200 MHz Intel XScale PXA2 chip with 16MB of Flash memory. The flash memory allows for program to be stored there for quick and easy access by the processor at bootup. The board has one 60-pin connector and a 92-pin connector to attach the additional expansion boards.

The Robostix has 8 sets of header pins for analog-to-digital conversion. The A/D converter has a 10-bit resolution and a conversion time between 13 and 260 μ s. The digital output resolution using the ADXL203 accelerometer is 0.9765 mV at 10-bits. For the ADXRS300 gyro, the digital output resolution is 4.39 mV at 10-bits. The A/D converters have a free running mode where they will constantly sample and update the ADC Data Register. This is done by writing a logical one to the ADSC bit in ADCSRA register of the microcontroller on the expansion board. However, the first conversion must be started by writing a logical one to the ADSC of the ADCSRA register. A program called i2c-io, gives the Gumstix the ability to read the Robostix's A/D conversions. When the input board is attached to the Gumstix, registers can be read by typing the command "i2c-addr Get port.pin", where the port is ADC and the pin is 0 through 7. This command is written in the Linux terminal and the 10-bit value is printed. The 10-bit value will be taken in by the C++ program and stored in the memory.

The data that is taken from the Robostix is stored on a CF card that is attached to the compact flash board. It interfaces with the Gumstix processor via the 92-pin connector. This provides the memory for data storage of the accelerometers and gyroscope outputs after the A/D conversion. The compact flash also serves as data storage for results from additional calculations that are made (algorithms, distances). Since the processor is running Linux, the CF card will be seen as storage device drive. In C++, code was written to store the data into a file such as a text document.

The Gumstix boards can be powered by a 5 volt A/C Adaptor or by batteries. The recommended voltage is between 4 to 5 volts because higher voltages cause heating issues in the processor. When interfacing with the host computer to upload code to the Gumstix, the 5 volt A/C Adaptor can be used. When the unit is being tested and it is necessary to be mobile, batteries can be used.

5.2 Software

After the team had a comfortable handle of the programming, positioning software algorithms were developed. A majority of these algorithms use basic principles of physics and calculus. For instance (assuming constant acceleration and constant velocity):

position (X) is found by:

$$X = x_0 + v_0t + .5*a*t^2$$

velocity (v) is calculated by:

$$v = v_0 + a*t$$

x_0 = initial displacement

v_0 = initial velocity

a = acceleration

t = time

Using these principles a two dimensional position system can be acquired. Once the team successfully modeled the equations to find positioning the software was downloaded to the processor and initial testing of the unit went underway.

Each step in the software has three separate programs that process the data that is coming in. The gyroscope, X-axis, and Y-axis of the accelerometer each go through their own specific programs. They do not get incorporated together until the final step where final positioning is calculated.

The compiler used to compile the C++ code is located in the buildroot for the Gumstix. It utilizes the uClibc libraries which contains a small C standard library. The intended use for uClibc is for embedded Linux systems like the Gumstix. A makefile, provided by Gumstix, directs the host computer to use uClibc to cross compile the C++ code for the Gumstix.

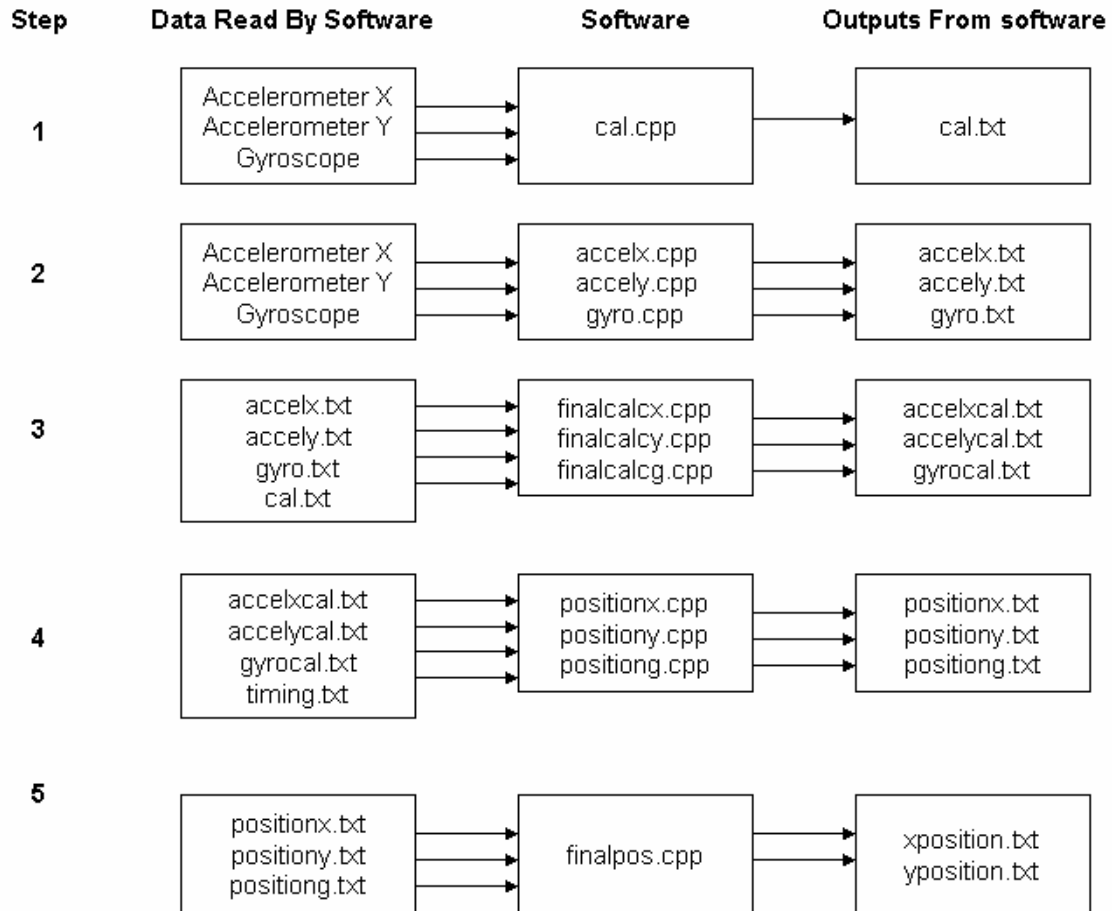


Figure 18: Software Flowchart

5.2.1 Step 1

The first step is for the software to calibrate the accelerometer and gyroscope. The software takes 50 data points from the gyroscope and averages them together to get the DC bias. An additional 50 data points are taken by the software for the accelerometers and the DC bias for the X-axis and Y-axis. These averages are stored in the file called cal.txt.

Scale factor, also known as sensitivity, is the ratio of change in the output due to a change in the input. Scale factor is expressed in V/g (volts per g, gravitational acceleration). Bias, also known as zero offset, is the average output of the sensor over a period of time which is measured at specific operating conditions which is not associated with the input. Bias is expressed in volts. Both of these two factors related to both

internal and external factors. Scale factor and bias can be calculated by the following formulas:

$$\text{Scale factor SF} = (V_{+g} - V_{-g})/2 \text{ V/g}$$

$$\text{Bias B} = (V_{+g} + V_{-g})/2 \text{ V}$$

V_{+g} is the voltage when the accelerometer is aligned with gravity

V_{-g} is the voltage when the accelerometer is 180° from gravity

Once these two factors are calculated acceleration can now be expressed by the following equation:

$$A = (V_o - B)/SF \text{ g}$$

Where V_o is the output voltage

In essence, the calibration that is applied is determining the bias at which it base all further calculations from.

5.2.2 Step 2

The accelerometer and gyroscope output voltages that correspond to acceleration and rate of rotation respectively. The software takes the data and uses analog-to-digital (AD) converters to convert the voltages into a digital representation. The AD converters can represent up to 5 volts with 10 bits. The software takes the binary bits and converts it into decimal form. Therefore, 0 volts is equal to 0 and 5 volts is equal to 1023. The programs then store the decimal voltage representations into text files called accelx.txt, accely.txt, and gyro.txt.

5.2.3 Step 3

The data is then taken and converted into voltages by multiplying the digitally represented voltages by .0048876. This number is 5/1023 which gives how many volts per decimal value. Once the converted number is obtained, the calibration data is used. The gyroscope and accelerometer calibration voltages are subtracted from the corresponding voltages gathered in step 2. This removes the bias from the components' output and brings the center voltage to 0V. By doing this, forward movements are positive and backward movements are negative for the accelerometer. The gyroscope

will have positive values for clockwise motion and negative values for counter-clockwise motion. This data is then stored into accelxcal.txt, accelycal.txt, and gyrocal.txt.

5.2.4 Step 4

In this step, the distances and degrees between each time interval are determined. First, the data is read into the software. A threshold is implemented in the accelerometer programs because there is a lot of noise coming from the accelerometers. There has been random noise up to $.2 \text{ m/s}^2$. A majority of the noise seen was below $.15 \text{ m/s}^2$. Therefore a threshold of $.15 \text{ m/s}^2$ was put into practice. This lowers the resolution of the system as a whole because it will not detect any acceleration below $.15 \text{ m/s}^2$. However, the system is capable of sampling at 6 samples per second; it is not enough resolution to distinguish the difference between noise and actual acceleration. When data is taken that is below $.15 \text{ m/s}^2$, it will be replaced with 0 m/s^2 . The time interval is calculated by taking the current time of the sample and subtracting it from the time of the next sample.

The accelerometer data is taken from the accelxcal.txt and accelycal.txt. This is then integrated once to get velocity. Velocity is then stored into a variable to keep track of the current velocity. When there is a change in acceleration, it is integrated to get velocity and is then added to the current velocity. The current velocity is then integrated to calculate the distance traveled during that time interval. This data is stored into positionx.txt and positiony.txt.

The gyroscope has a conversion of $12.5\text{mV}/^\circ/\text{s}$. When the voltage from the gyroscope is taken and divided by $12.5\text{mV}/^\circ/\text{s}$, the result is $^\circ/\text{s}$. It is then multiplied by the time interval to determine the degrees that the system has moved. The current degree status is stored into a variable to keep track of the rotation of the unit. The current degree rotation is stored into positiong.txt.

5.2.5 Step 5

In the final software, all the distances in the X-axis and Y-axis, and current gyroscope rotation were taken into account. By taking the X-axis distance and the Y-axis distance and using arctangent, theta can be determined. When theta and the gyroscope degree rotation are added together, this provides Phi, the total angle of the position vector P.

Position vector P is calculated with use of the Pythagorean Theorem, X-axis and Y-axis distances. Using the trigonometry functions sine and cosine, positioning, relative to the original direction that the unit was placed is calculated for each time interval. After each data point, it is added to the current location of the IMU to show the position of the system at each data point. These values are stored in the files xposition.txt and yposition.txt. At the end of the program, the final positioning is output to the screen in HyperTerminal.

5.2.6 Software Changes and Additions

One issue in the software that the team experienced was recognizing if the unit was stationary or moving at constant velocity when the accelerometers were outputting zero acceleration. The accelerometers output acceleration when it experiences acceleration, but returns to the DC bias when it does not experience any acceleration, however the unit may be moving at a constant velocity. In order to determine the current status of the system at zero acceleration, velocity must be kept in memory. When the accelerometers experience acceleration, it is integrated into velocity and is added to the current velocity. Positive acceleration leads to adding a positive velocity to the current one. Negative acceleration adds a negative velocity to the current velocity. Therefore, if equal but opposite accelerations are felt by the accelerometers one after the other, the velocity will go up and then go back down the same amount and be at zero velocity when there is no acceleration. If the accelerations were not equal and opposite, the velocity will be at a constant velocity when the accelerometer is not experiencing any acceleration.

Software was added to implement start and stop buttons. The buttons are connected to AD converters and 5V. The software will wait until the start button is pressed before the program begins calibration. When the stop button is pressed, the unit stops gathering data and begins processing it. The stop button functionality has been disabled because for testing purposes, it is easier to have a specific amount of data points for different tests.

5.2.7 Software Validation

Several different tests were done to validate the integrity of the software. Simulated data were put into the text files accelx.txt, accely.txt, gyro.txt, and timing.txt. This data was input as digital voltage representation in decimal form. The timing increased at intervals of one second. The values were taken and then simulated in the program to determine if the correct outputs were achieved during each step of the programs. The values were also calculated by hand to validate the proper outputs.

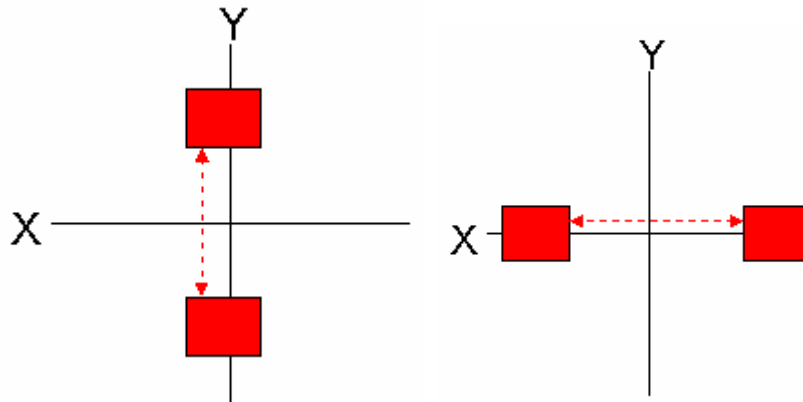


Figure 19: Software Validation - Movement in X and Y Axes - No Rotation

The system was simulated to move along each axis to determine whether the algorithms were written correctly without rotation of the gyroscope. It was simulated to move forward and backwards along the Y-axis to make sure the software worked in both cases. The same was done to the X-axis.

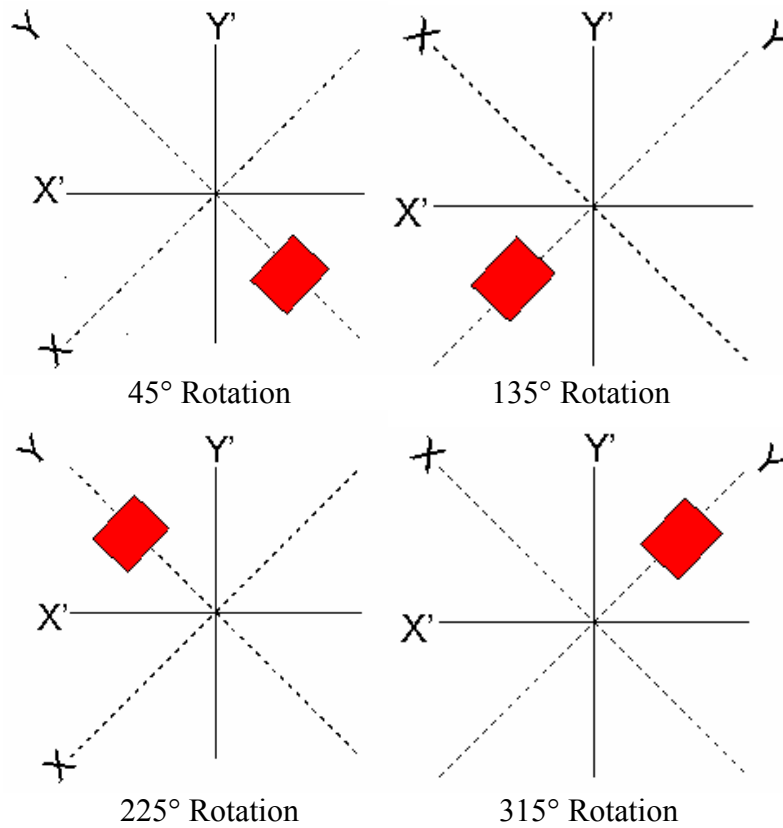


Figure 20: Software Validation - Rotation and Movement in Y Direction

The data simulated that the system rotated and then moved into each of the quadrants shown in Figure 20. This was done in four different tests to eliminate any errors that could occur in previous steps. This was important to determine whether or not the system would be able to understand the trigonometry functions and determine which quadrant it is currently located in. When using the tangent function, certain negative signs are lost due to the characteristics of the tangent. When using tangent, the system without correction software would produce the same outputs when the system went in the positive X direction and positive Y direction and when the system went in the negative X and negative Y direction.

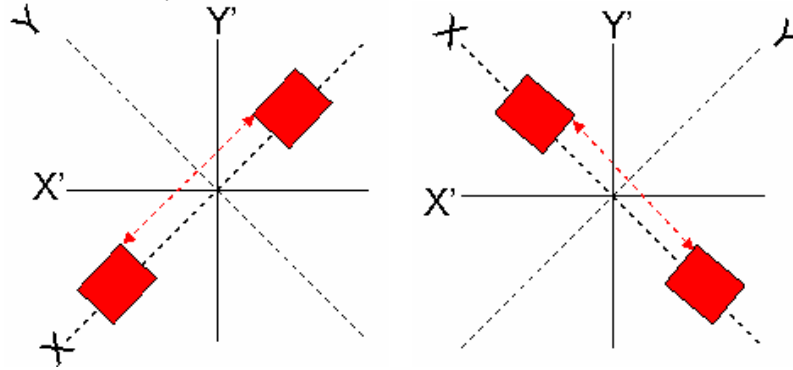


Figure 21: Software Validation - Rotation and Movement in X Direction

In these software test verifications, the unit was rotated and then accelerated back and forth along the axis. This was used to validate that the trigonometry was correctly implemented in the software.

After completing the software validation, initial testing could be done with confidence that the system is accurately using the input data and calculating positioning.

5.3 System Functionality

When the inertial measurement unit (IMU) is powered on, the operating system boots up. Once the operating system is booted, it automatically begins running the script which contains instructions on which part of the program to run at what time. All of the data is then stored onto the compact flash card, see Figure 18.

The first part of the program is calibrating the sensors. The system waits until the start button is pressed before it begins calibration. Calibration consists of two steps – calibrating the gyroscope, then calibrating the accelerometers. During the gyroscope calibration, the unit is completely still. This allows the system to determine the initial bias by averaging several data points. The accelerometer calibration is done in the same manner. The calibration data is stored into a text file.

The IMU begins gathering data immediately after calibration finished. Initially, the unit checks to see how many data points to take by checking a file stored on the compact flash card. This number can be changed to meet testing requirements. The data gathered by the A/D converter consists of the bit representation of voltages from the accelerometer for the X and Y-axis and from the gyroscope. Each time the system

gathers data for the accelerometer and gyroscope, it has a corresponding timestamp. All of the data is stored in separate text files.

Immediately following the data collection, the filtering is applied. This consists of converting the bit representation of the voltages into voltages and removing the initial bias of the MEMs sensors' data. The software looks into the calibration text file to determine the bias. It centers the data around 0 so forward motion is positive and backward motion is negative for the accelerometer in its corresponding axis. This data is then stored into three different text files for the accelerometer X-axis, accelerometer Y-axis, and gyroscope.

Lastly, the script runs the positioning software. The distance is determined by integrating the acceleration twice, between each time interval. To solve for the rotation of the unit, the data from the gyroscope is taken, divided by the sensitivity ($12.5\text{mV}/^\circ/\text{s}$), and multiplied by the time interval. This gives the degrees of rotation of the unit. These values are stored into separate text files. From there, the positioning software uses trigonometry to determine the location of the device at each time interval.

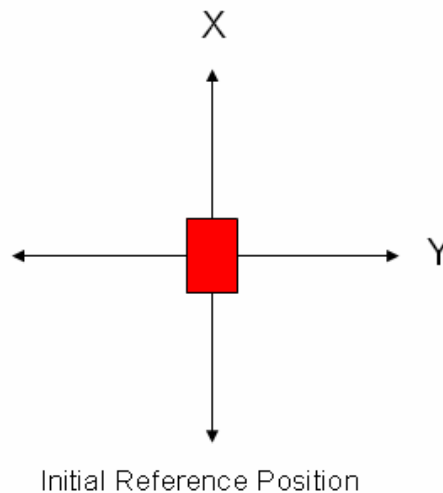


Figure 22: Step 1 - Initial Reference Position

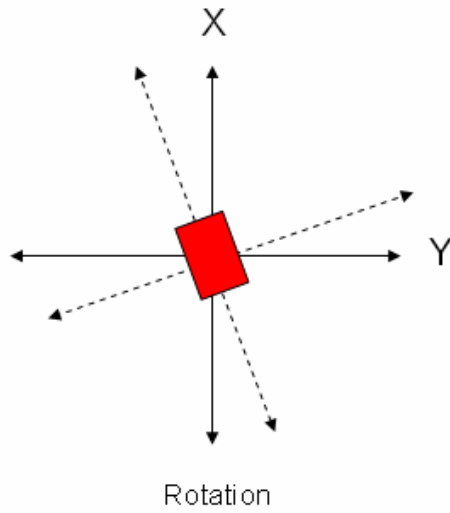
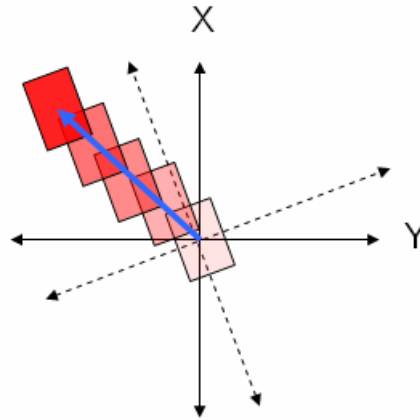
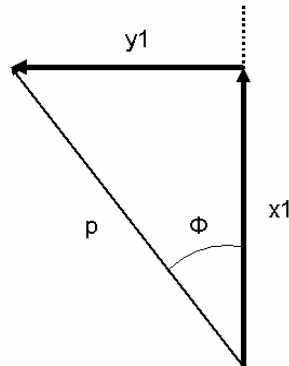
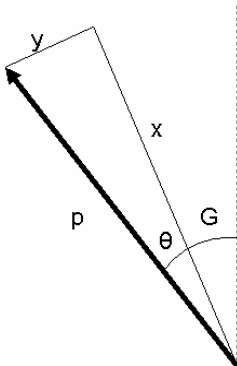


Figure 23: Step 2 Rotation of Unit



Movement in the X and Y Axes

Figure 24: Step 3 - Unit Movement



Given:

X = Accel position X-axis

Y = Accel position Y-axis

G = Gyro degree

Calculated:

$$\theta = \tan^{-1} (Y/X)$$

$$\Phi = \theta + G$$

$$P = \sqrt{x^2+y^2}$$

$$Y1 = P*\sin(\Phi)$$

$$X1 = P*\cos(\Phi)$$

Figure 25: Step 5 - Calculations

When the system begins the data acquisition, the initial reference position is taken and the final position is relative to the reference (Figure 22). The unit then rotates by G degrees (Figure 23: Step 2 Rotation of Unit). It then stays at that rotation and moves along the blue line P (Figure 24: Step 3 - Unit Movement).

The acceleration in the X direction and Y direction are known. The integration of these parameters will result in the position vectors relative to the rotation of the unit. The results would be the variables X and Y in Figure 25: Step 5 - Calculations. Using the Pythagorean Theorem, the final positioning vector P can be found. θ is calculated by using arctangent of Y/X . Another parameter that is known is the rotation of the unit, G . When θ and G are added together, the degree rotation is referenced to the original position of the unit when the data acquisition began. By knowing Φ , the total rotation relative to the original position, and P , $X1$ and $Y1$ components relative to the original position can be found. This is done by $Y1 = P*\sin(\Phi)$ and $X1 = P*\cos(\Phi)$. If the system is connected to a computer through HyperTerminal, the final coordinates are displayed on the screen in meters. The processing of the data takes approximately 2 seconds to complete before the data is displayed on the screen.

5.4 Operational Modes

The unit works in two different modes. The unit can work as a stand alone system or be connected to the PC via serial cable. In stand alone mode, the unit is battery powered and stores the data and processed data to the compact flash card. The IMU will be free roaming. This allows for testing to be done where more motion is required. The data can then be received using a compact flash card reader and connecting it to a PC. When the system is connected to a PC, it can be powered by either battery or the AC adapter. Testing is limited to the length of the serial cable. The final positioning will be shown on the screen.

6 Testing and Results

Both the accelerometers and gyroscopes were tested individually as their outputs need to be analyzed separately so that software can be written to filter out noise and drift.

Each sensor was evaluated for one axis orientation, after one axis was explored a two dimensional system was observed.

6.1 Test Plan

Test verification is very important because it provides proof of functionality of the project. A method of test verification is comparing the ideal outcomes with actual outcomes. This can only be done when all the variables can be controlled and a known outcome can be determined. If the device is functioning properly, the actual outcome should be very close to the ideal outcome.

After the software was validated, testing of the sensors could now commence. Five different types of tests were completed in order to ensure complete testing of the gyroscope and the accelerometers. These included stationary testing, rotary stage testing, one-dimensional testing on each axis, two-dimensional testing, and additional testing to compare the sensors to their specifications. Multiple tests had to be taken in order to achieve conclusive results. Testing was considered complete if the results, whether accurate or not, could be repeated.

6.2 Stationary

Stationary testing is required in order to analyze the bias at which the sensors output when at rest. Analysis of the deviation from the bias would give some detailed information on the drift rate and/or noise of the system. The accelerometers are ratiometric, meaning the output bias level voltage is a ratio of the input voltage to the sensor. In this case the bias level of these sensors is half the input so a 5 volt input voltage would result in a bias of 2.5 volts. The gyroscope is not ratiometric however its bias according to the datasheet should be at a constant 2.5 volts. It is important to know what the bias levels are in order to properly base output voltages from them.

The stationary testing did not require any additional equipment in order to run the tests. A flat surface and a computer to interface with was all that was needed. Approximately one minute of data collection, 250 data points, was taken for each test. First calibration was completed, then after triggering the start button the data was collected. After each test was completed the data was stored for further analysis. The

initial set of stationary tests was run multiple times. However the output values were wide in variation. At times the team would see movement as low as 1 meter during the one minute test and other times we would see 60 meters of movement. Figure 26 is an example of one of the initial tests run. The final position was $X = 13.11262$ meters and $Y = -38.8474$ meters. While expecting $X = 0$ and $Y = 0$, this output was clearly experiencing major noise and/or drift, and was proof to how sensitive these sensors really are.

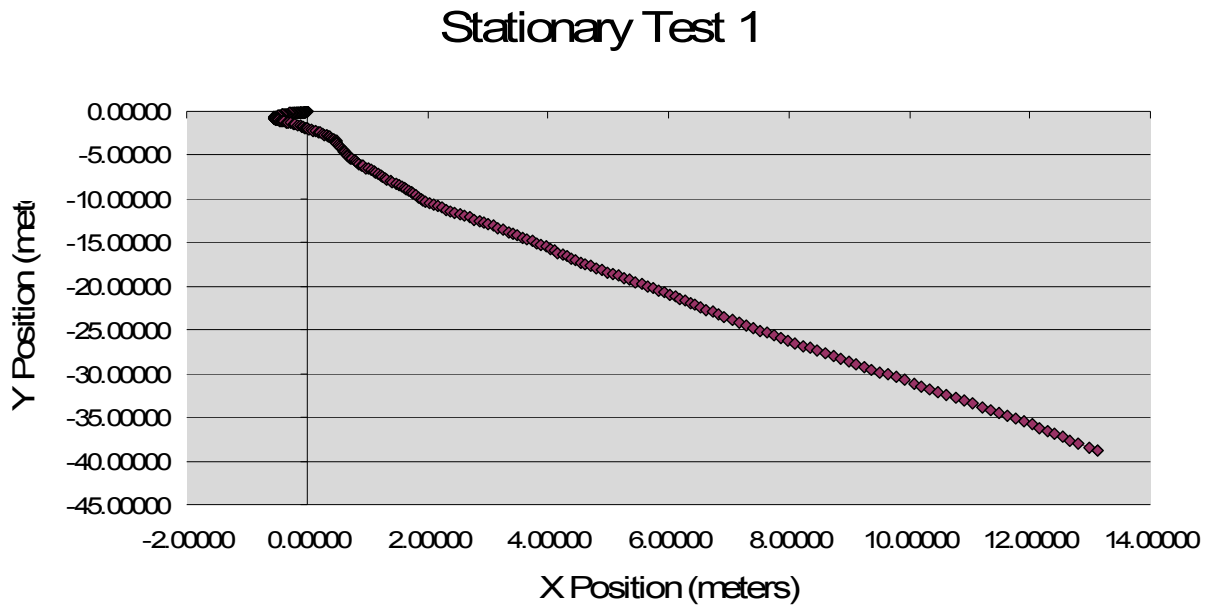


Figure 26: Stationary Data in Initial Test

Further analysis of the test results was needed in order to make a conclusion as to why the sensors were experiencing this amount of movement. With varying stationary outputs such as those in Figure 26 and others that have shown movement in both the positive and negative in both axes, no distinct evaluation could be made except for the fact that the output was random.

Due to the fact that the unit was not moved physically it was apparent that the outputs were caused due to some error in the system that was unforeseen. Capacitors were put into place to limit the noise on the output. In order to remedy the additional

noise that the sensors were encountering, a software threshold was applied. Analysis of the test results concluded that much of the noise seen was between 0 and 0.015 m/s^2 . The threshold was set to “ignore” any acceleration in this range so the outputs would not be affected by this source of error. Figure 27 shows the output of the sensors after the threshold was applied. The final position of this test was $X = 1.09986$ meters and $Y = 1.64457$ meters, a result that was more expected. Additional tests using the threshold yielded results with much higher accuracy, our highest accuracy showing (0,0) and our lowest accuracy still showing less than 5 meters in either axis.

Stationary Data With Filtering

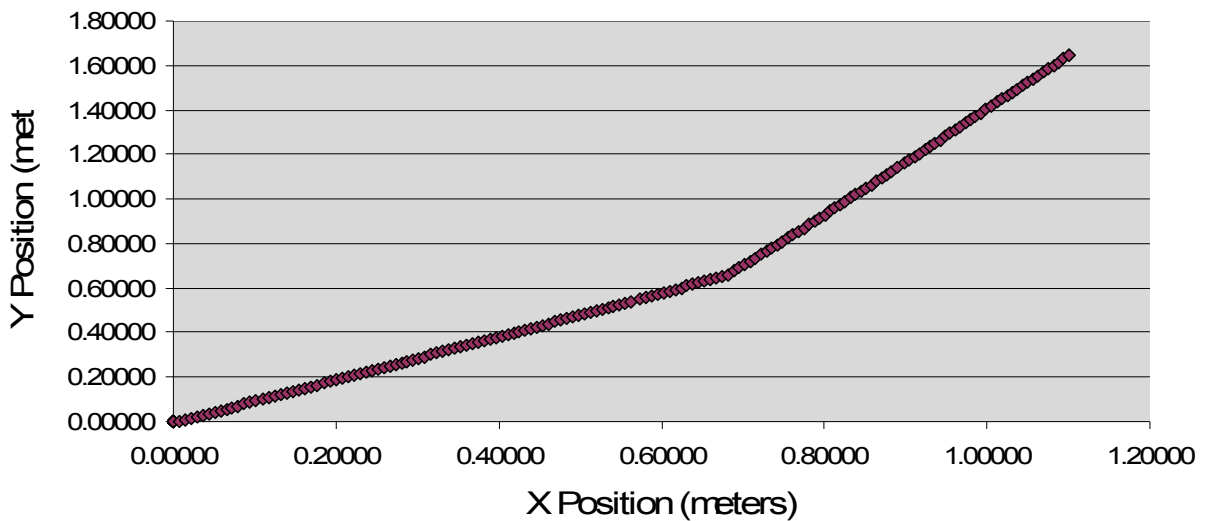


Figure 27: Stationary Test with Threshold Filtering

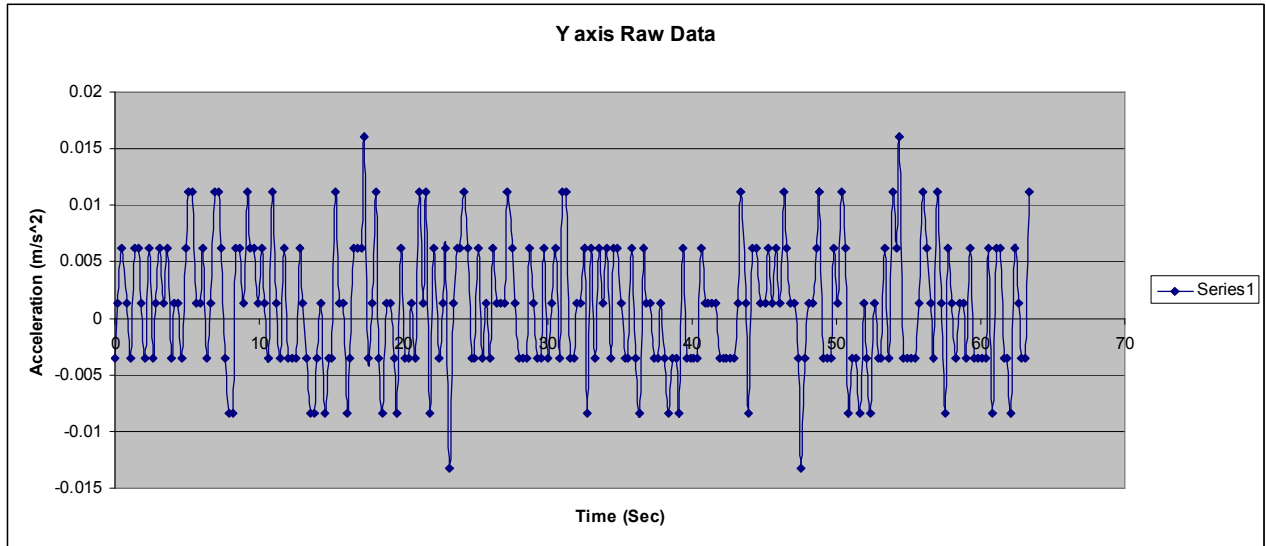


Figure 28: Test 3 Y-Axis Acceleration

It was necessary to examine the raw data from the accelerometers in order to determine whether the drift that was now seen even after filtering was caused from mechanical drift or calculated drift. Figure 28 is a graph of the Y-axis test 3 of Table 5. Almost all of the data points fell within the threshold, however there were two points during the test that exceeded it. These two points resulted in the calculated drift in the final position because the software assumed it was an applied acceleration. However it was not an acceleration, just a spike in the noise. Graphs such as this proved that the error seen in these tests was due to calculated drift, from the double integration of a noise spike. This is discussed in a later section.

Further analysis revealed an additional source of error. The system, due to its slow sampling rate, was experiencing aliasing effects. Meaning, the analog signal (from the sensors) is being sampled improperly so when it is reconstructed from digital to analog we are losing some key components of the original signal. In order to remedy this effect the sampling rate of the sensors must be at least twice the frequency in which they are outputting data. Luckily the bandwidth on each of the sensors can simply be adjusted by adding additional capacitors to create low pass filters. Since the A/D converter samples around 6 Hz the sensor bandwidth must be limited to at most 3 Hz so the nyquist criterion is satisfied. A bandwidth of 1 Hz was decided upon. In the ADXL203 data sheet a table of bandwidths is given with corresponding capacitor values. For a 1 Hz

bandwidth a 4.7 uF capacitor is needed between both the X-axis rate out and the Y-axis rate out. For the gyroscope simple calculations are needed to find the corresponding capacitor value. In the ADSRS150 data sheet the following equation is provided:

$$f_{OUT} = 1 / (2 \times \pi \times R_{OUT} \times C_{OUT})$$

With $f_{out} = 1$ and the data sheet states $R_{out} = 180 \text{ K}\Omega$ that makes $C_{out} = .88 \text{ uF}$. The needed capacitors were obtained and placed accordingly.

With the noise threshold set and the aliasing resolved a set of 15 stationary data collections was completed. The results of these tests are summarized in Table 5.

Test	X Final Position	Y Final Position	Gyro Final Degree
1	0.000	0.000	1.71477
2	-0.00001	0.000	2.32843
3	-0.21626	2.16446	7.51689
4	0.21407	1.89577	-9.39405
5	-0.02879	0.97474	2.53040
6	0.822340	2.415108	1.743650
7	-0.000008	0.000	-2.582086
8	-0.000027	-0.000001	1.669407
9	2.577790	0.157705	7.488987
10	-0.000004	0.000	-2.797097
11	1.197604	0.007033	-5.818635
12	-0.028986	4.461288	1.629695
13	4.024572	1.347391	-9.156627
14	1.153845	1.583025	-6.019371
15	-0.000003	0.000	3.997300

Table 5: Stationary Data Collection Results

The results conclude that even with the noise threshold the sensors still see additional noise. It is also clear that the calculated drift can occur in any direction depending on where the noise exceeds the threshold. Thus making it impossible to try and account for calculated drift prior to testing. The average calculated drift in the X-axis is 0.684 meters for the 1 minute span of data collection and the average calculated drift in the Y-axis is 1.0004 meters. That is 0.0114 m/s and .01667 m/s, respectively.

Unlike the accelerometers the gyro never experiences zero movement according to the test results. The average calculated drift in the gyro is 4.4278 degrees for the one minute test meaning 0.0738 degrees per second. This is within the range of the specifications for the gyro. According to the data sheet the gyro will drift less than .2 degrees/sec with an accuracy of 0.02 degrees. Figure 29 shows raw output of the gyro when stationary. Like the accelerometer there is no apparent drift. However due to a spike in the noise, this leads to a calculated error in the positioning.

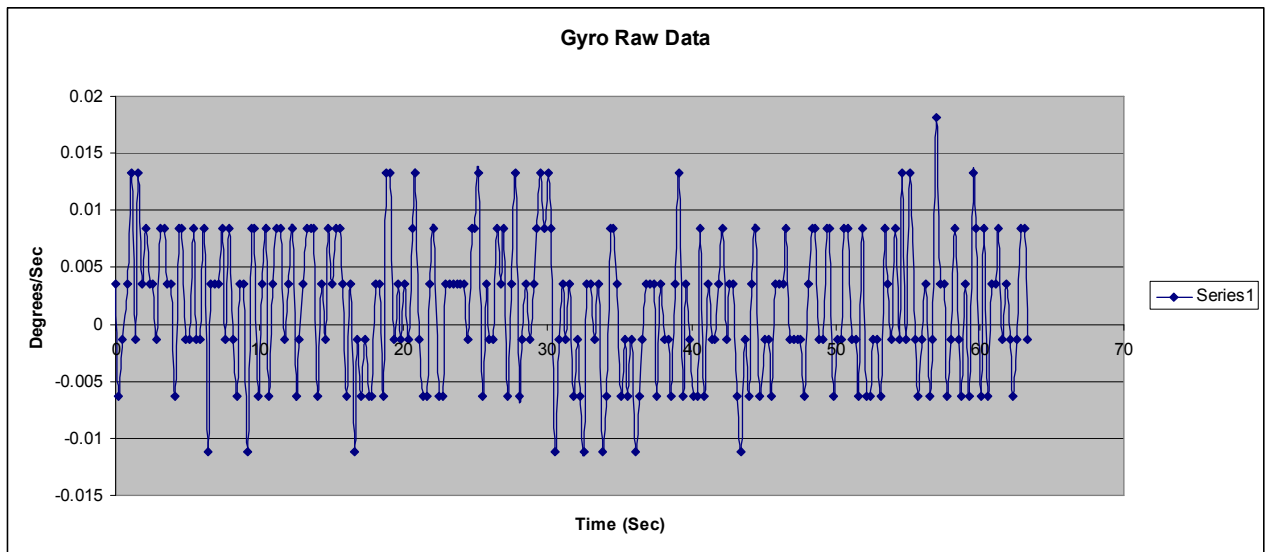


Figure 29: Gyro Raw Data – Stationary

The graphs below show X-axis, Y-axis and gyro movement versus time during test 5. This is just to give the reader a visual look into the sensor outputs during stationary testing.

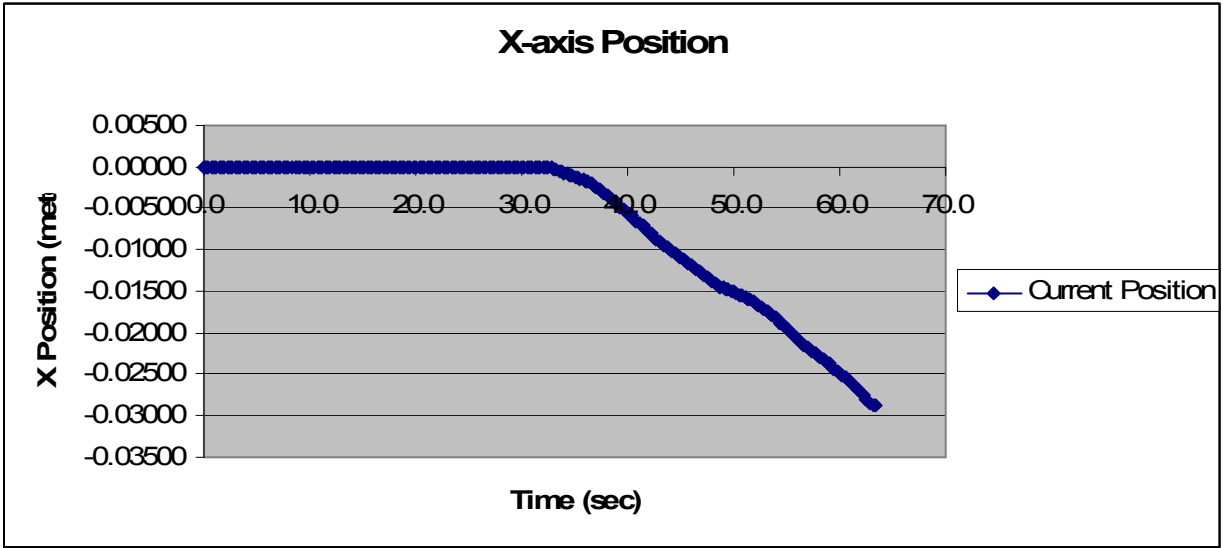


Figure 30: Stationary Test 5 X-axis vs Time

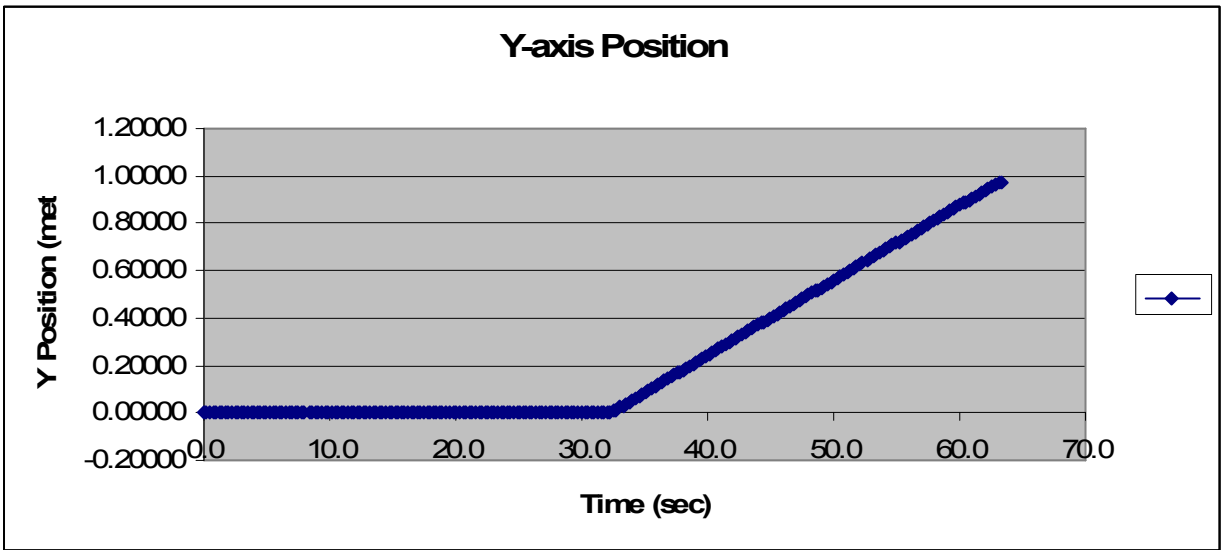


Figure 31: Stationary Test 5 Y-axis vs Time

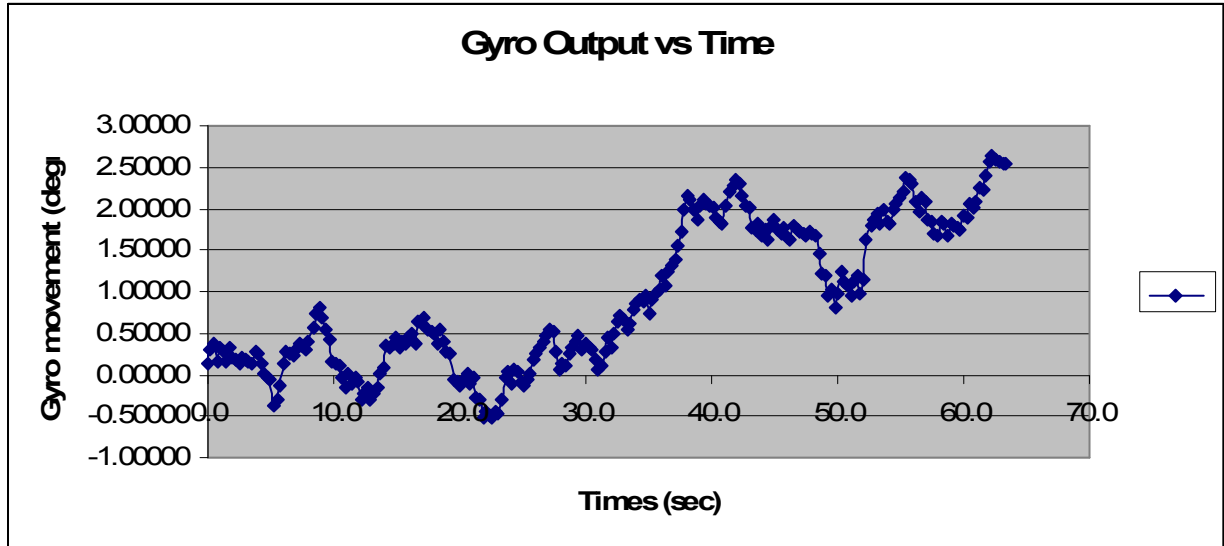


Figure 32: Stationary Test 5 Gyro Degrees vs Time

A portion of the error in final positioning is due to mathematical round off error during position calculations. Even though the error that is rounded is minimal, when it is integrated twice (from acceleration to displacement) these errors accumulate in a much larger fashion. Understanding such concepts is crucial when considering what applications this unit may be used for.

6.3 Rotary Stage Testing

Rotary stage testing was needed to ensure proper functioning of the gyroscope. An SR50 Series Compact High-Resolution Rotation Stage (see Figure 33), manufactured by Newport Corporation, located in the CHSLT (Center for Holographic Studies and Laser micro-mechaTronics) lab in the WPI Mechanical Engineering department was used for this test. This stage has an absolute accuracy of .035 degrees and can rotate up to a maximum of 4 degrees per second.



Figure 33: SR50 Series Rotary Stage⁴⁰

For this set of tests we rotated the unit both positive and negative 90 degrees at a rate of 2 degrees per second. We pre-set the stage to move 90 degrees automatically then stop. The data was stored for later analysis. Then the stage was moved a negative 90 degrees and that data was stored. Both sets of tests were needed to confirm that the gyro was correctly sensing positive and negative rotations. In Table 6 a summary of the testing data can be found.

Test	Expected Final degrees	Actual Final degrees
1	-90	-88.72871
2	90	100.7575180
3	-90	-80.44445
4	90	96.1966220
5	-90	-75.95476
6	90	88.7434840
7	-90	-93.73247
8	90	84.2346730
9	-90	-85.71607
10	90	92.9918280

Table 6: Rate Table Output Summary

Table 6 displays the final rotation seen after 300 data points were taken. However on multiple tests the final rotation deviated from the maximum rotation experienced. For instance in test 8 the gyro did “see” 90 degrees, however once the stage stopped rotating the gyro started to drift back down to 88.7 degrees. Figure 34 shows how the gyro outputs begin to drift. Looking at the data more closely the gyro is registering a rotation of approximately 2 degrees per second, the rate at which the stage is moving, so the gyro is correctly sensing the rotation to which it is being subjected to.

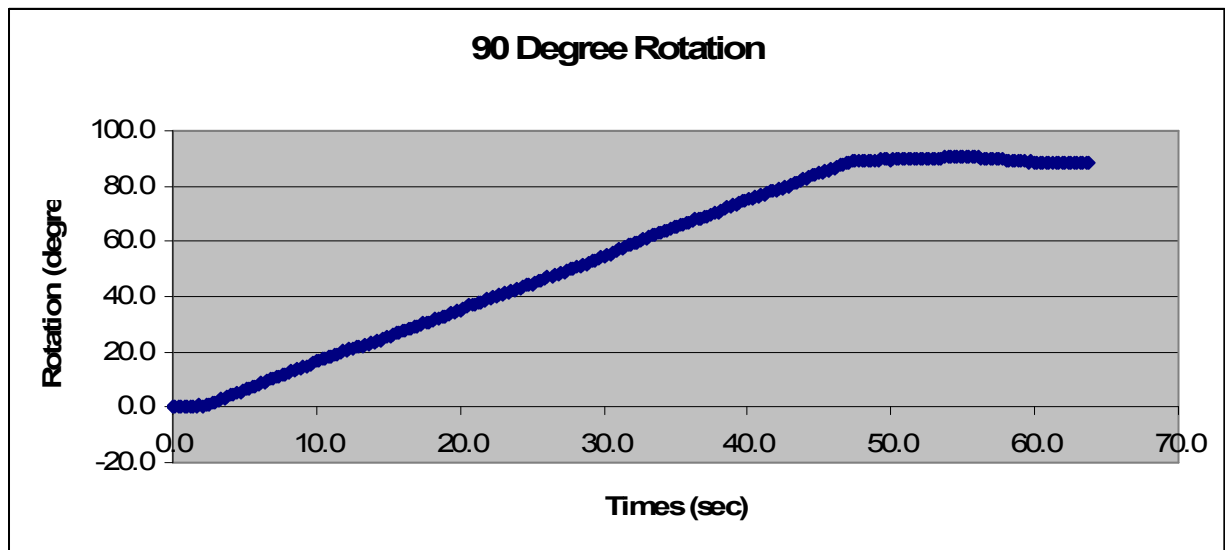


Figure 34: Test 8: 90 Degree Rotation

The largest percent error seen while taking the rotation tests was during test 5, with an error of 15.6%. Like the scenario explained earlier, this test also deviated from the maximum degree of rotation. At the time when the stage stopped the gyro had seen a rotation of -81.18071 degrees, making the gyro measurement during rotation be within the specified accuracy. Figure 35 is a graph of test 5, Rotation vs Time. In spite of this all of the other rotary tests were within the 14% error. Although it would have been beneficial to include rotations greater than 90 degrees, the system is limited in the number of data points that can be collected during a single test. Due to the fact that the software limits the size of the data arrays, and the speed at which the stage can rotate, additional degrees of rotation were omitted. Overall, this test was conclusive and we are now confident that the unit can properly detect positive and negative rotations.

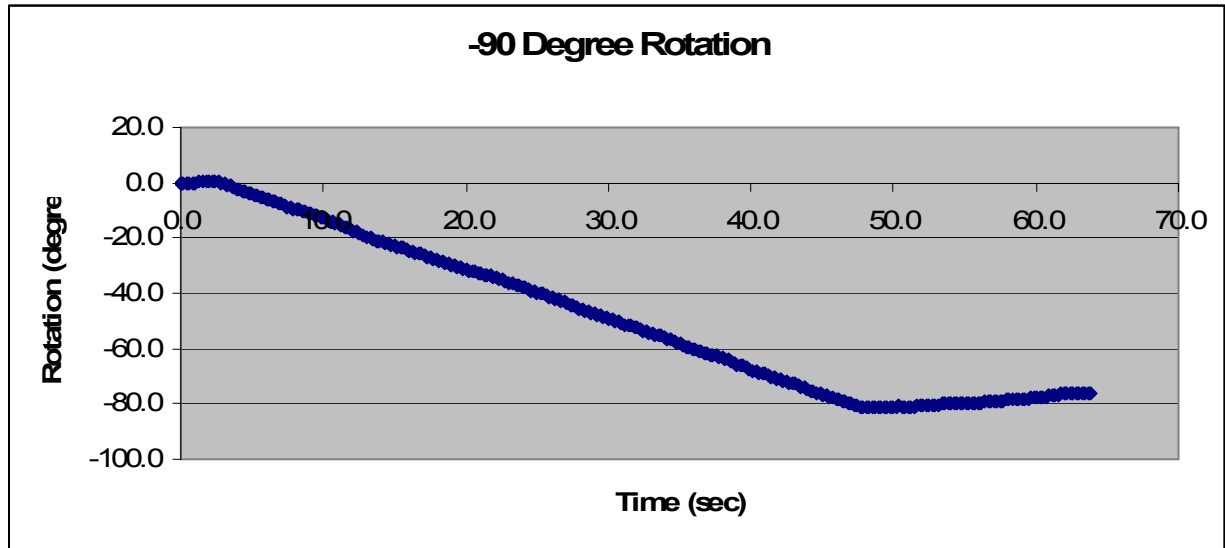


Figure 35: Test 5: -90 degree rotation

6.4 One-Dimensional

One-dimensional testing was needed to ensure proper detection of movement on both the X and Y axes of the accelerometer. In order to complete such tests, equipment from Vernier Software and technology was needed. There were four main pieces of equipment needed, a motion detector, a cart, a track and corresponding software.

The motion detector uses ultrasound technology to measure distance traveled by the cart. The detector pulses a beam of ultrasound, and the time it takes for the pulse to hit the cart and return to the device is used to calculate position. With such devices however, the pulse may reflect off nearby objects as well, so it was important to keep other objects away from the testing area. The unit was placed onto a low friction Vernier cart. Depending on which axis was to be tested the unit could be placed accordingly. The cart was then placed on a Pasco Scientific track that measured 227 cm (a tape measure on the track could be used for visual measurements). With the motion detector at one end, the cart (and unit) could be moved up and down the track to be measured.

Vernier Lab Pro, Logger Pro v. 3.4.5 software was used in conjunction with the motion detector to give a real time graph of the unit moving up and down the track. While position was gathered both velocity and acceleration were differentiated, however due to the errors in rounding, the acceleration given by the software was steady around 0

m/s². However the position of the cart was the important data to be retrieved from this test.

Tests were completed for all four movement options with the unit; \pm X-axis movement and \pm Y-axis movement. The tests took approximately 10 seconds, so 50 data points were needed for each test. Table 7 is the compiled results from the one-dimensional testing.

Test	Expected X Final Position	Actual X Final Position	Expected Y Final Position	Actual Y Final Position
1	1.05918	1.16038	0	-0.31213
2	1.061928	0.58839	0	1.11700
3	0.965888	0.51752	0	0.25410
4	1.056715	1.15592	0	0.36282
5	-1.171139	-1.16119	0	-0.13594
6	-1.114339	-1.14245	0	-0.39100
7	-1.145071	1.26142	0	0.68877
8	-1.041348	-1.18705	0	-0.02730
9	0	-0.68119	.95793	1.02471
10	0	0.24124	.941036	0.22436
11	0	2.23994	.958753	-1.00174
12	0	0.60942	-1.170828	-1.16827
13	0	-0.11610	-1.280076	-3.08291
14	0	1.46459	-1.206811	-2.17393

Table 7: 1-Dimensional Testing Results

Analysis of these results yields the greatest percent error in the X-axis (during movement) to be 44% during test 3 and the greatest percent error in the Y-axis to be 141% during test 13, which is unacceptable. However, we are able to get values with only 0.8% error. It is possible that during movement there was vibration of the cart leading to some of the errors. It is also possible that some tilting may have been

experienced leading to the sensors “thinking” it was accelerating faster than it actually was. These results conclude that it is possible to get reasonable position with the sensors. Errors that were seen on the axis not under test could be due to calculated drift because it is stationary or it is possible that if the unit was not placed precisely to only provide motion to the current axis under test then some motion may have been experienced on both the X and Y axes. Figure 36 shows the accelerometer outputs versus time and Figure 37 shows the Logger Pro software outputs. Figure 37 shows the start position at $X = 1.493285$ meters and the final position at $X = 0.322146$ meters with a total distance moved of -1.171139 meters. The two graphs show the correlation between the units positioning system and the Logger Pro’s position software.

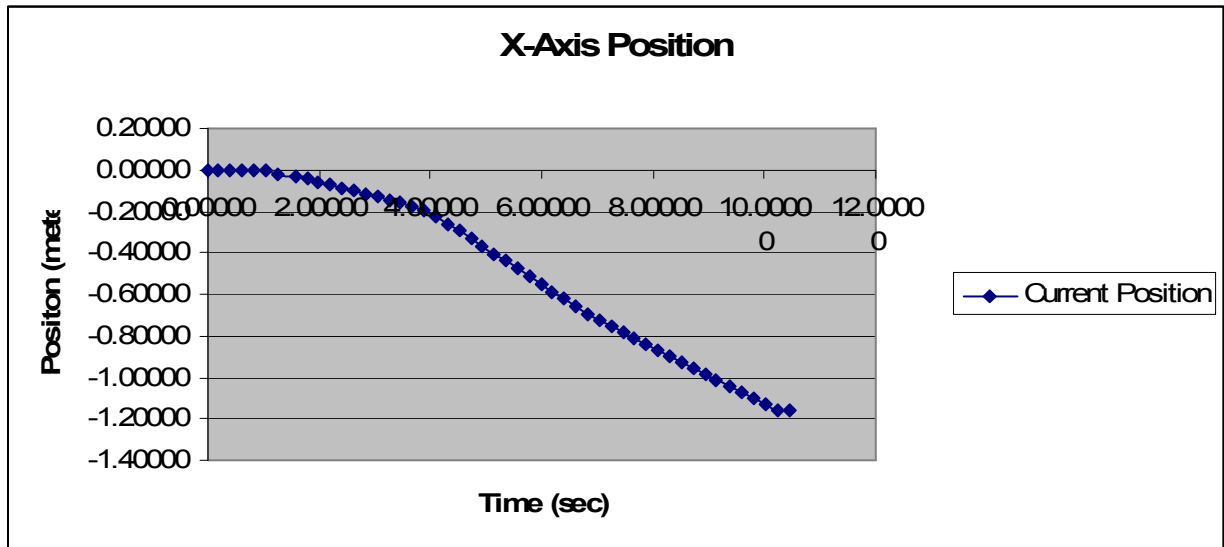


Figure 36: Test 5 X-Axis Movement seen by Accelerometer

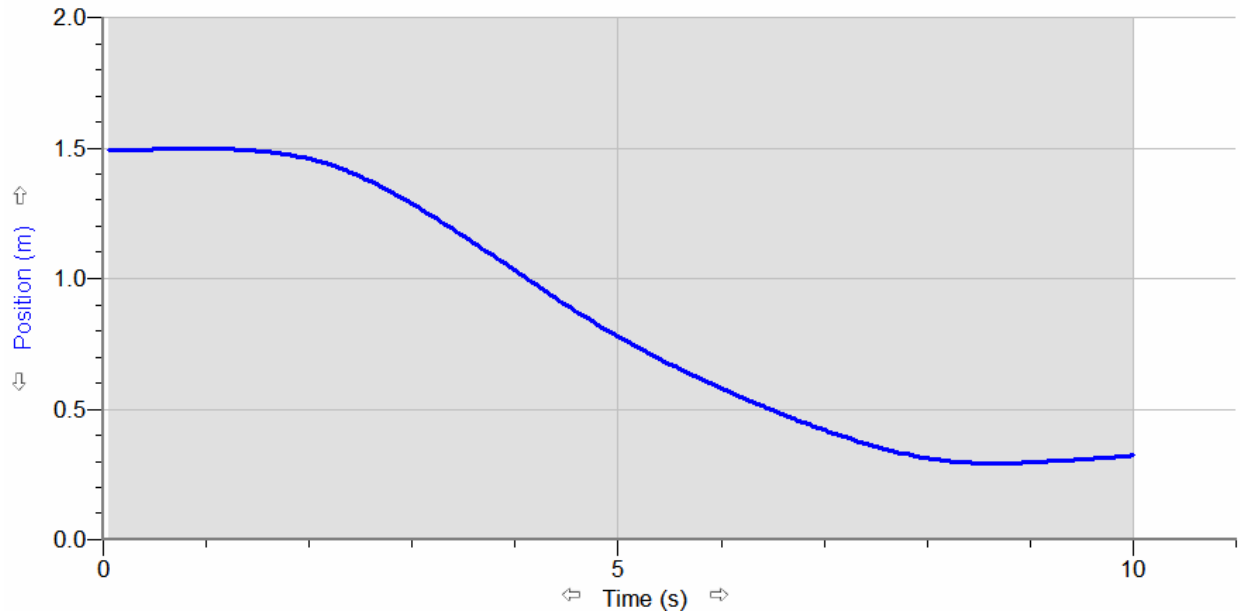


Figure 37: Position Seen by Logger Pro Software and Vernier Equipment

6.5 Two-Dimensional

Two dimensional testing was done to determine how the unit functions when there is motion in both axes. This was done using a cart with wheels. A laptop and the unit were placed on the cart and were then moved in set directions and distances. There were several different tests that were done on the unit.

The first test consisted of moving the unit 0.91 meters in the X-direction and -0.91 meters in the Y-axis simultaneously. Fifty data points were taken for this test to have time before and after the movements to observe if there was any type of drift that deviated from the threshold.

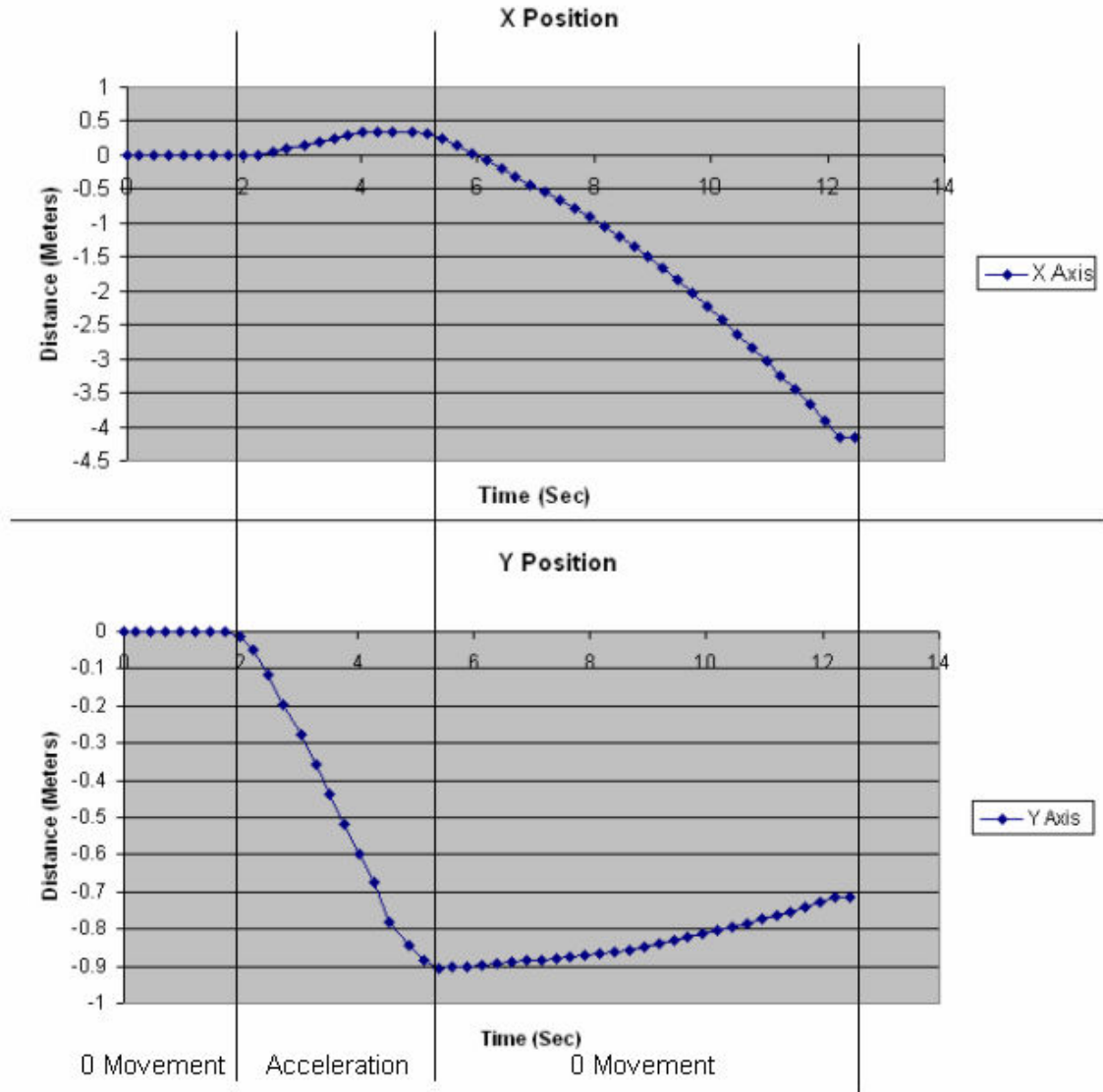


Figure 38: Simultaneous X and Y axes movement

The unit's calculated final positioning was -4.15 meters in the X direction and -0.714 meters in the Y direction. By observing the graphs, the unit stayed stable before any movement was made, then the components sensed motion in the correct directions. After the unit stopped moving, calculated drift due to noise began to take over. Viewing the raw data after the unit had stopped it was apparent that the noise exceeded the threshold, creating false accelerations. The drift had affected the X-axis more than the Y-axis. Before the drift, the Y-axis observed -0.9 meters of movement when the actual movement was -0.91 meters. However, the X-axis only observed 0.4 meters and the noise spikes pulled the results to negative values.

Another test that was performed was moving the unit in a square.

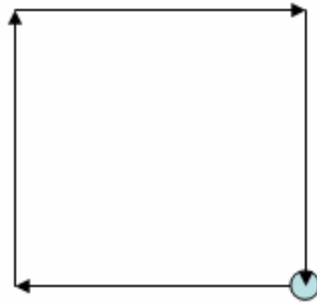


Figure 39: Unit Movement in 2D Testing

This test was done to see if the unit would calculate that it had moved a total displacement of zero meters in both of the axes.

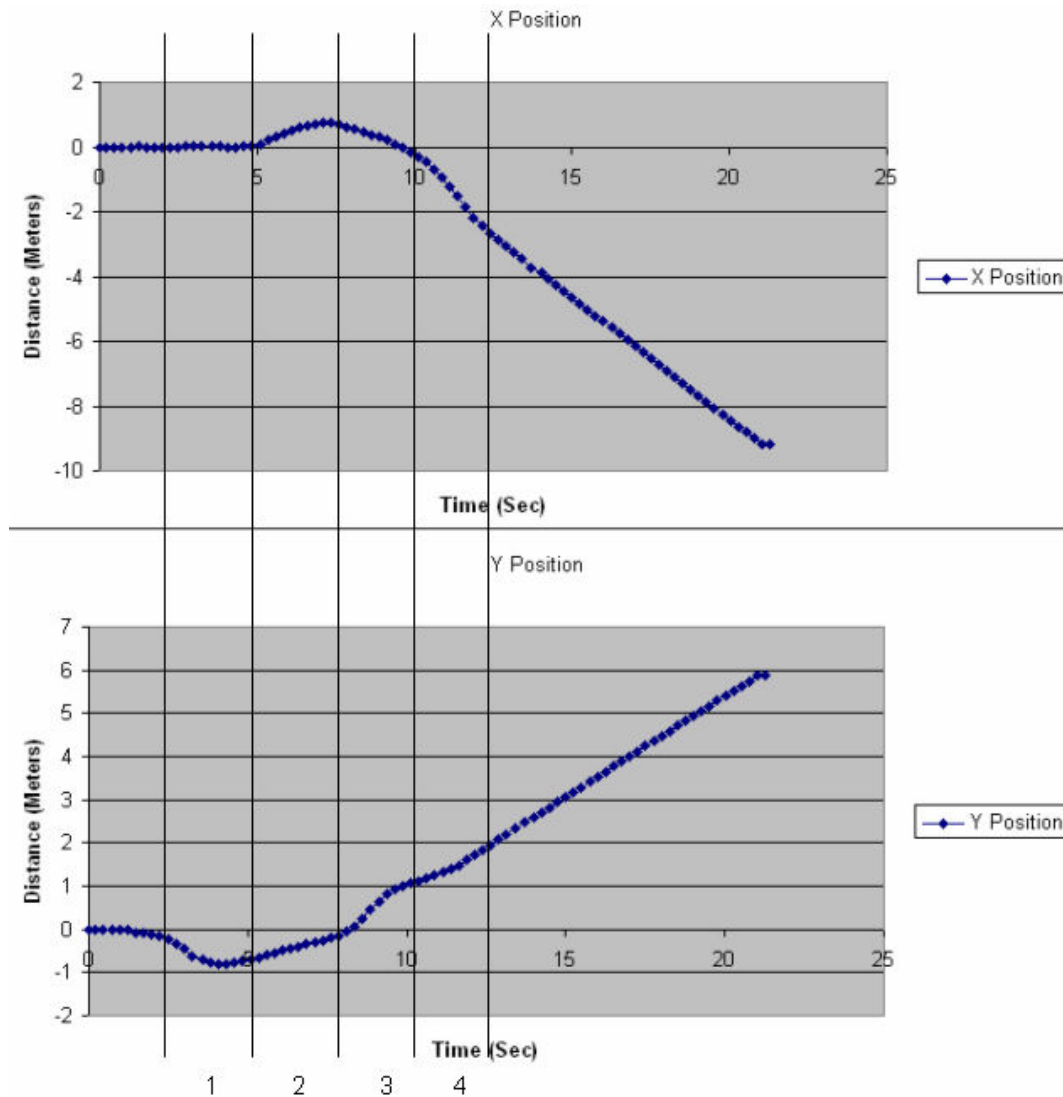


Figure 40: Square 2D Test Data Points

In section 1 of the graph in Figure 40: Square 2D Test Data Points, the unit moves in the Y-axis for -.91 meters. The X-axis stays very close to zero. In section 2, the IMU then moves in the positive X direction for .91 meters. In this section, the Y-axis begins to drift in the positive direction. In section 3, the Y-axis moves in the positive direction. However, the drift from section 2 made the calculations start from roughly 0 meters instead of -.91 meters. The Y-axis calculations did compute 1 meter of movement in this section. In section 4, the unit then experienced acceleration in the negative X direction. The acceleration detected by the accelerometer was not as accurate and provided greater acceleration than there actually amount. This made the calculation show -2.3 meters in the X direction rather than -.91 meters. After section 4, the noise spikes sent the calculations further into the negative X direction and positive Y direction. The final calculation was -9.2 meters in the X direction and 5.9 meters in the Y direction.

Test	Expected X Final Position	Actual X Final Position	Expected Y Final Position	Actual Y Final Position
	(Meters)	(Meters)	(Meters)	(Meters)
1	0.91	-2.72564	-0.91	-2.601
2	-0.91	0.967676	0.91	1.56474
3	0.91	-4.14731	-0.91	-0.7138
4	-0.91	0.110045	-91	1.00805
5	0.91	-0.49959	-0.91	-1.0026
6	-0.91	-0.89406	0.91	0.30127
7	1.82	-3.09254	-0.91	0.92499
8	-1.82	-0.34287	0.91	4.97325
9	-0.91	-3.86579	-0.91	0.84072
10	-0.91	2.581777	0.91	-0.5911
11	0	-10.9875	0	1.52258
12	0	-5.89317	0	9.13806
13	0	-17.814	0	1.58804
14	0	-9.19892	0	5.86668

Square 0
Displacement

Table 8: 2-Dimensional Testing Results

Analysis of the 2-Dimensional testing resulted in a greatest percent error in the X-axis being 356% from test 3. The greatest percent error in the Y-axis is 446% in test 8. However, the greatest distance the calculations were off by was in test 13 for the X-axis and test 12 for the Y-axis. These tests were the longest test run and had the most

movement. Vibrations could have been the leading cause for the sensors to output erroneous accelerations. The Y-axis was much more consistent and stable compared to the X-axis.

6.6 Error Analysis

After analyzing the results from the stationary, 1-D, 2-D and rotary testing it was clear that there were some sources of error causing the inaccuracies of the final output. In order to determine where these errors originated from additional analysis had to be completed. This brought the team back to the stationary data. Initially the thresholding provided more accurate results, however, it was hiding the error instead of compensating for it. It was also limiting the resolution of the system, by ignoring any actual accelerations occurring within the threshold range.

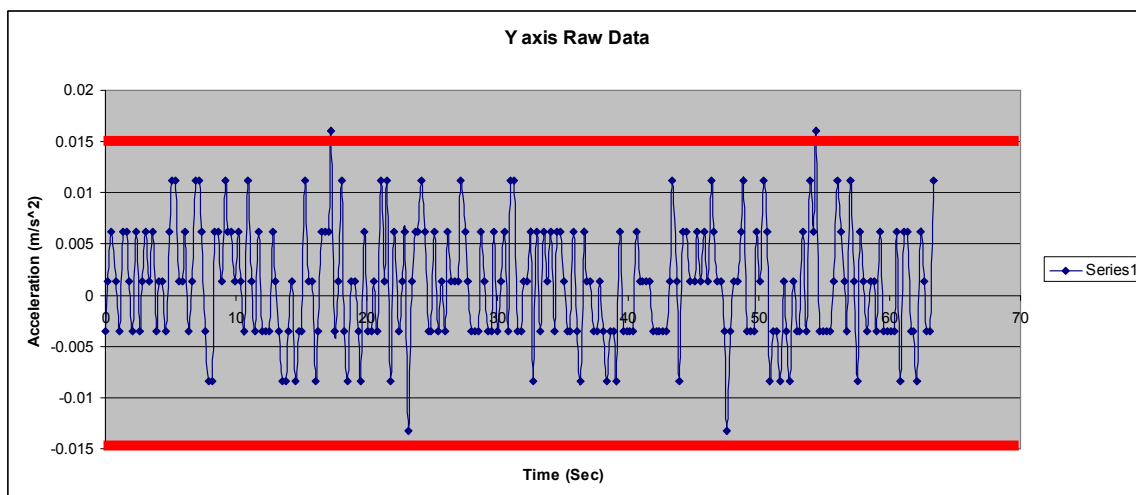


Figure 41: Noise Spike Outside Threshold Range

Figure 41 is a graph showing the red lines which represent the threshold boundaries. It is noticeable that there are two points of noise that exceed this boundary. This causes the system to calculate position using false accelerations. This leads to inaccurate final positioning because the two points transfer to two constant positive velocities. Since thresholding was now no longer a viable solution, it was removed from the software.

The next possible source of error that was investigated was calibration. For the current system setup, calibration is completed with the initial 50 data points taken during step 1 of the software process. This results in the initial 0 G bias. In order to determine if

the bias was accurate, a new bias was calculated by averaging an entire data set of stationary data. This can only be done with stationary data because it is known that the entire data should be bases around 0 with no accelerations. Once this was done there was a difference in the biases based on the two different means of calculating them.

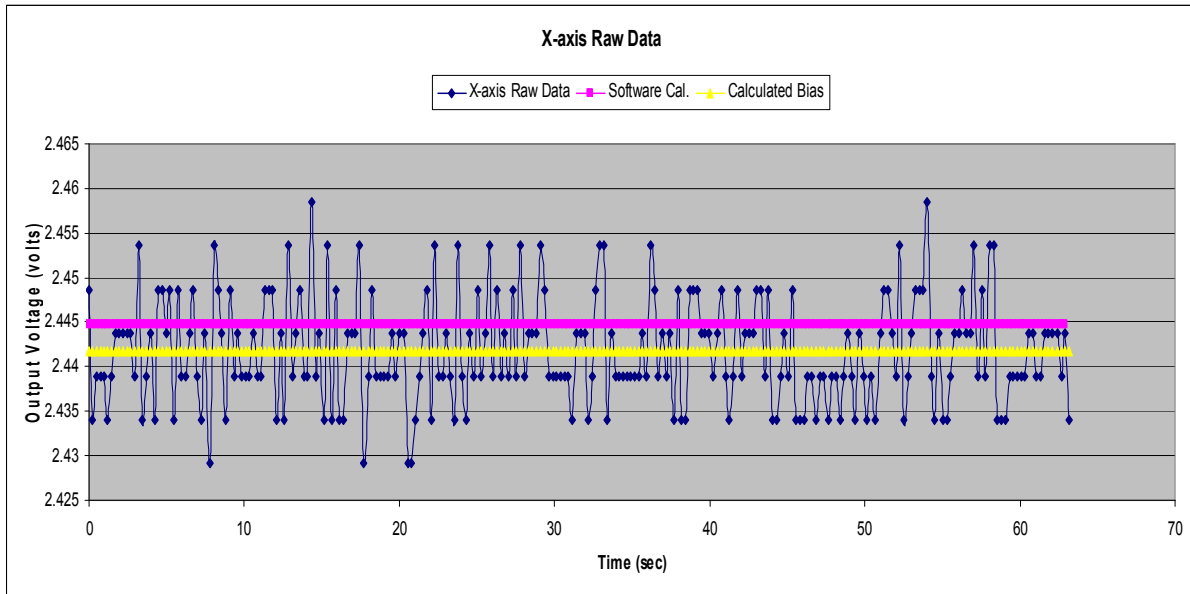


Figure 42: Bias Calibration

In Figure 42, the pink line indicates the bias calculated during the software procedure and the yellow line indicates the bias calculated by averaging the entire data set. Although these lines have a small deviation from each other, 2.93 mV, this difference leads to a large difference in final position.

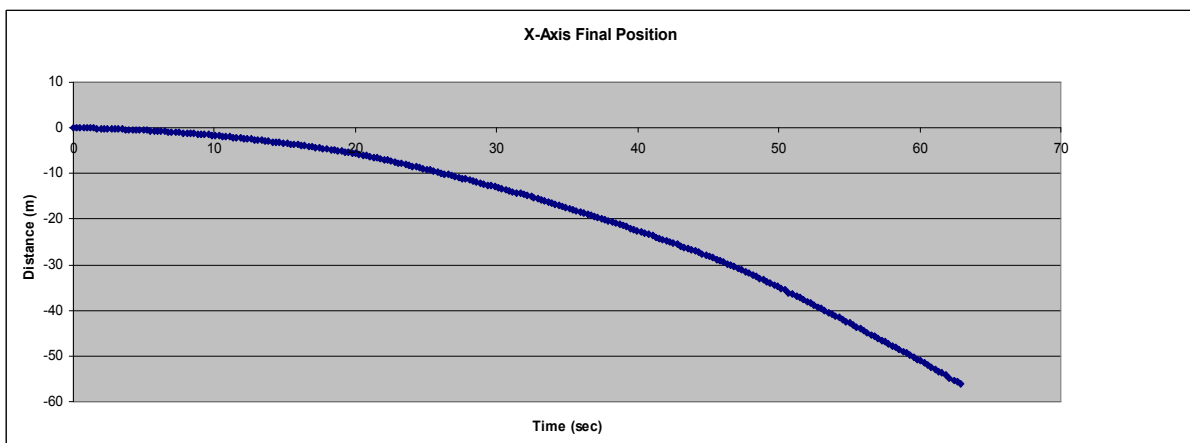


Figure 43: Final Postion with Software Calculated Bias

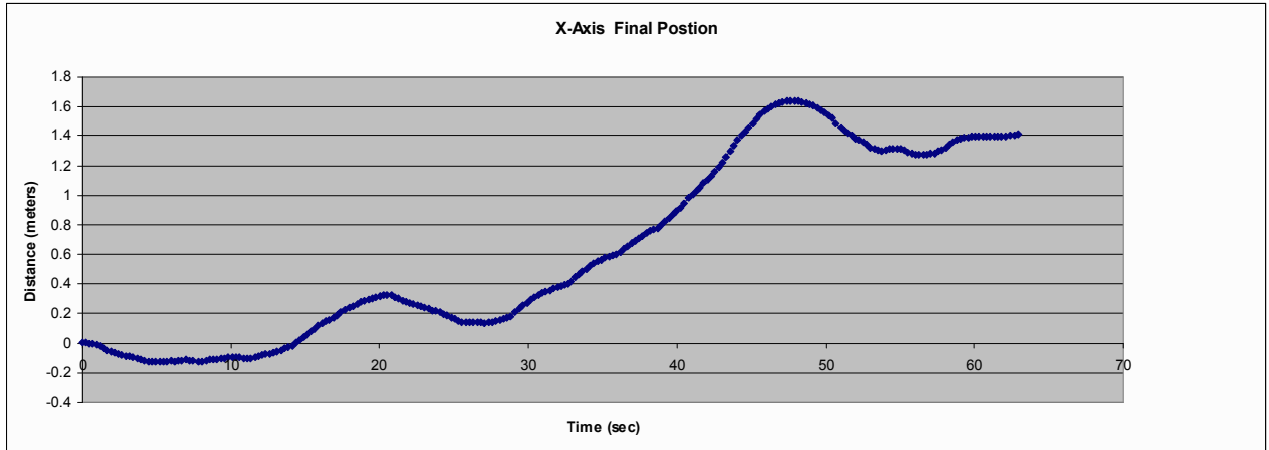


Figure 44: Final Position with Averaged Data Set Bias

Figure 43 has a final position of -53.197 meters and Figure 44 has a final position of 1.407 meters. This proves that accurate calibration is needed in order to obtain a higher degree of accuracy on the final output. The data shows that millivolts in deviation cause tens of meters of final positioning error.

In order to determine how often recalibration is needed to keep a certain degree of accuracy, 250 data points were averaged in 50 point intervals. In doing so the team hoped to see a steady increase or decrease that would allow the team to determine at what point to recalibrate to bring the bias back to 0. However Figure 45, Figure 46 and Figure 47 show that there is no steady increase or decrease, the bias levels jump up and down making it hard to see a trend. As seen in previous tests the bias can deviate from the actual by approximately 3mV. By recalibrating every 50 data points, approximately every 8 seconds the team is able to increase the accuracy of the final position from a test from 2.31 to -0.136 meters. In another test the final output changed from -5.809 to 0.358 meters using the same method. This is another drastic increase in accuracy from the prior calibration technique.

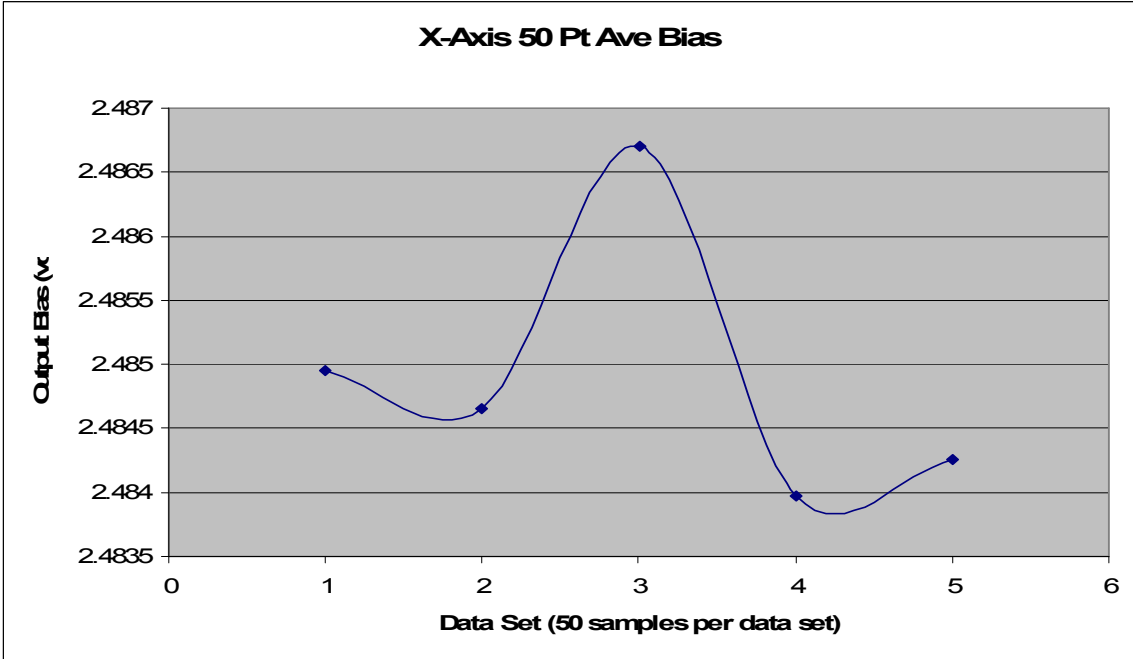


Figure 45: 50 point Averaged Test 1 Accelerometr

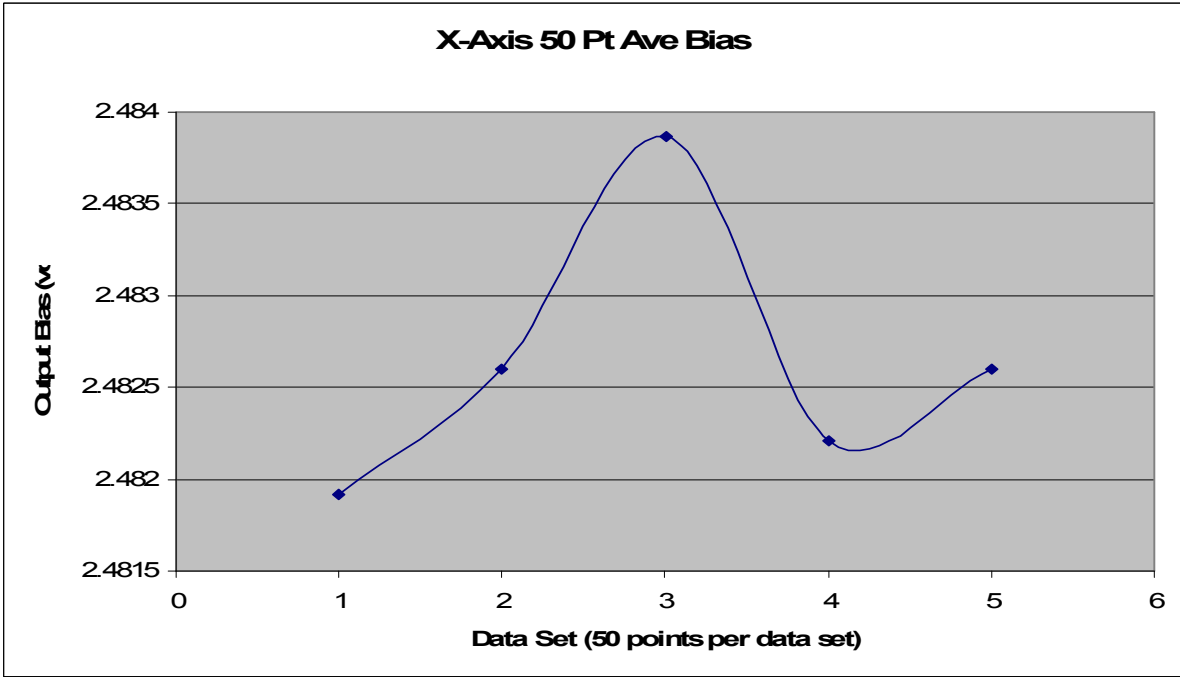


Figure 46: 50 Point Averaged Test 2 Accelerometer

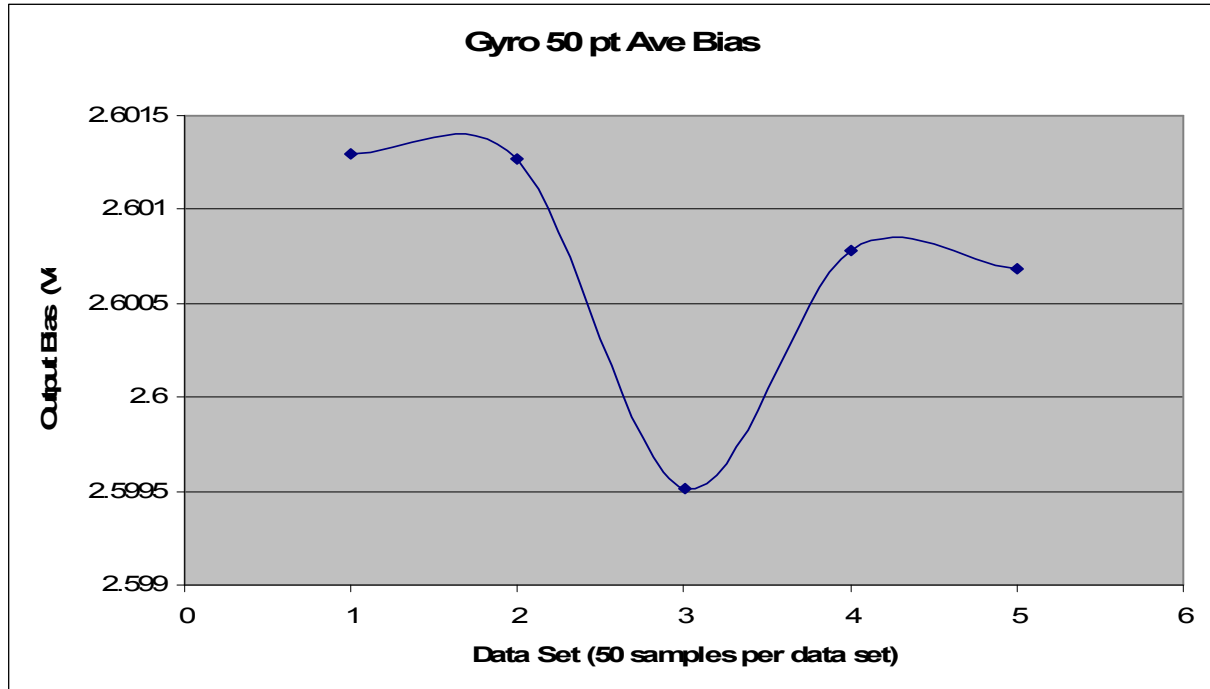


Figure 47: 50 Point Averaged Gyroscope

Another source of error could be the timing intervals at which the data was being taken. The average time interval for the system was .165 seconds. The timing interval was off by at most 1 ms. Occasionally, there were times when the system would take .26 seconds to gather data. Noise in the system should be completely random and essentially cancel each other out over the bias point. However, this produced errors when the system was computing the integrals for displacement and rotation because the time intervals were not exactly the same. This caused some noise to last longer than others and not cancel each other out.

When writing software in C++, it is very difficult to have software run code at specific time intervals. When writing code at such a high level, it is easier to understand. However, there is a lack of control over the processing. For more accurate timing, a micro controller is necessary, such as a PIC. When writing code in assembly, each line of code corresponds to a certain amount of clock cycles. This would be very valuable to know because each clock cycle will correspond to a specific amount of time. C++ does not have enough control over the processing to gather data at exact time intervals.

6.7 Sensor Specification Testing

Several tests were run to ensure that the sensors fell within the specifications of Analog Devices. Since the actual testing of the system proved that accurate final positioning could not be determined, it was important to verify that the sensors were working correctly. This is very important to do in order to gain a better understanding of the sensors and to be able to determine if the sensors are producing the correct outputs. Besides testing the sensors within the test bed, they were also tested separately on a breadboard using a voltage supply, multimeter and oscilloscope to view the outputs. This was done to eliminate any additional variable that might affect the outputs.

6.7.1 Accelerometer Zero g Bias Level

The specifications of the accelerometer state that the Zero g Bias level at a supply voltage of 5 V is typically 2.5 V and can have a maximum of 2.6 V and a minimum of 2.4 V. This test was completed by gathering 100 samples of data from each of the sensors. Two different accelerometers were tested to see the differences and similarities between sensors. The data was then analyzed and the minimum, maximum and average biases were taken.

Test 1		
	X-Axis	Y-Axis
Max	2.527	2.502
Min	2.497	2.468
Ave	2.512	2.483

Table 9: Accelerometer 1 Zero G Bias Level

Test 2		
	X-Axis	Y-Axis
Max	2.502	2.498
Min	2.473	2.468
Ave	2.488	2.485

Table 10: Accelerometer 2 Zero G Bias Level

The final results of the tests prove the accelerometers 0 G bias levels are within the specified range.

6.7.2 Accelerometer Temperature Variance

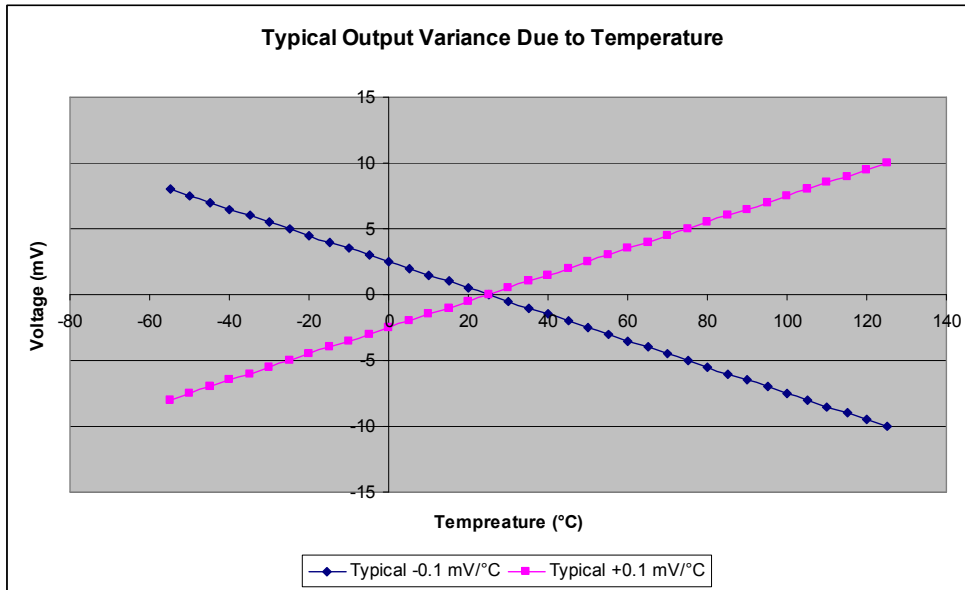


Figure 48: Typical Output Variance due to Temperature

The 0 g bias can vary depending on temperature. There is a typical variance of ± 0.1 mV per degree Centigrade. The graph above displays the typical variance that can occur within the operating range of -50°C to $+125^{\circ}\text{C}$. The typical variance can fall anywhere between the two lines at any given temperature. For instance, at 120°C , there can be a variance of anywhere between -10 mV and 10 mV from the actual output voltage corresponding to the acceleration. However, getting closer to 25°C (normal operating temperature), the variance becomes much less.

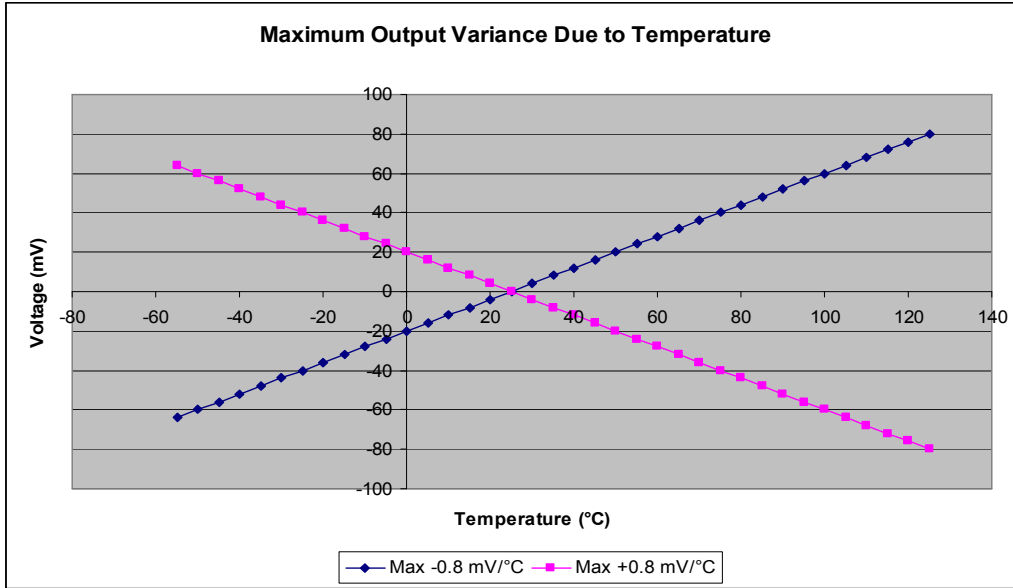


Figure 49: Maximum Output Variance due to Temperature

The above graph displays the maximum variance due to temperature. It is ± 0.8 mV per degree Centigrade. Without a means to control the temperature surrounding the sensors, this graph displays the variance that could be experienced by the output of the accelerometers due to temperature.

6.7.3 Accelerometer Sensitivity

At a supply voltage of 5V, the specifications are that the accelerometer will output between 960 and 1040 mV per g experienced. The typical value is 1000 mV per g. This test consisted of taking data for the 0 g bias, -1 g and +1 g. Gathering data for the -1 g and +1 g was accomplished by tilting the sensor to view its maximum and minimum values. Since the sensor is parallel with gravity, the sensor will experience the force of gravity, or ± 1 g, depending on which side of the axis is downwards.

1 g Testing Accelerometer 1		
	X-Axis	Y-Axis
-1g	3.49	1.46
0g	2.49	2.45
+1g	1.5	3.44

Table 11: Accelerometer 1, Sensitivity Test

1 g Testing Accelerometer 2		
	X-Axis	Y-Axis
-1g	1.48	1.47
0g	2.48	2.51
+1g	3.48	3.45

Table 12: Accelerometer 2 Sensitivity Test

After completing the test on both accelerometers, all of the results fell within the specifications of the sensors except for the Y-Axis accelerometer at +1 g. The range is ± 40 mV from the bias plus 1 V (1 V = +1 g). This sensor was 60 mV away from the actual value, being 3.45 V. This error could possibly be due to misalignment of the axis during manufacturing or temperature offset.

6.7.4 Gyroscope Zero Rotation Null Value

The null value for the gyroscope is the value at which the gyroscope outputs zero rotation. The typical value for this sensor is 2.5 V. The sensor that was used for this system had a null voltage of 2.57 V. This null value can be adjusted by adding resistors from pin 3 of the gyroscope evaluation board to ground or the voltage source. When connecting to ground, the null voltage increases. The voltage decreases when connecting to the voltage source. The resistor value needed can be found by using the following equation:

$$R_{\text{NULL}} = (2.5 \times 180,000) / (V_{\text{NULL0}} - V_{\text{NULL1}})$$

V_{NULL0} is the zero rotation output without any adjustments. V_{NULL1} is the desired null voltage of the sensor. Typical values for the null voltage resistor fall between 1 M Ω and 5 M Ω . In order for the sensor of the system to output 2.5 V, a calculated R_{NULL} value of 6.1 M Ω is required. This was done to the system to produce a zero rotation bias of 2.5 V.

6.7.5 Gyroscope Sensitivity

The sensitivity of the gyroscope is described by the amount of millivolts that correspond to one degree per second. This sensor has a typical sensitivity of 12.5 mV/ $^{\circ}$ /s. However, this can vary between 11.25 to 13.25 mV/ $^{\circ}$ /s. From the gyroscope

tests with the rotary stage, the sensitivity was determined. The rotary stage rotated at a constant 2°/s.

1°/s Sensitivity Test	
Zero Rotation Bias:	2.603519 V
-2°/s output:	2.580146 V
Difference:	.023374 V
-1°/s = .023374/2 =	11.687 mV/°/s

Table 13: Gyroscope Sensitivity Testing

The sensitivity of the sensor in the system is 11.687 mV/°/s. This is slightly lower than the typical value, but it falls within the range of minimum and maximum values.

6.7.6 Gyroscope Temperature Variance

The zero rotation bias of the gyroscope can vary depending on the temperature of the sensor. There is a temperature output on the gyroscope that outputs voltages that correspond to temperatures. It outputs 2.5 V at 27°C and has a proportional characteristic of 8.4 mV/°C. Below is a chart of a test from Analog Devices that monitors the output bias voltages at the full range of temperatures that the sensor can functionally operate in.

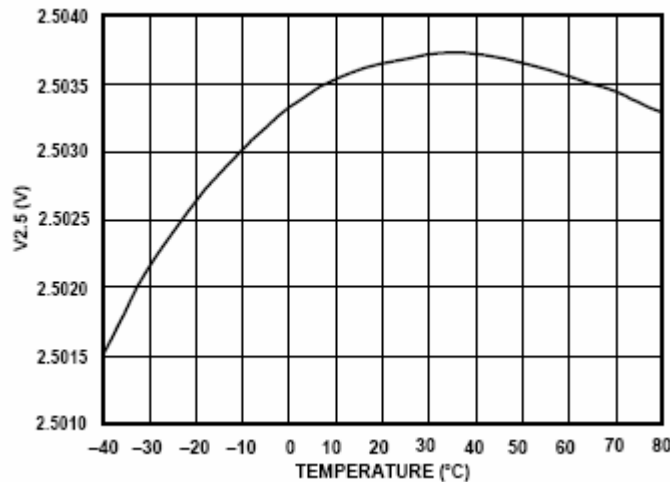


Figure 50: Gyro Output v Temperature⁴¹

By using a 3-point calibration technique on the null and sensitivity drift, Analog Devices states that the sensor can achieve an overall accuracy of 300°/hour. However, with a higher degree of calibration, an accuracy of 70°/hour can be achieved.

6.7.7 Gyroscope Self Test Response

The self test pins assure functionality of the sensor. There are two self test pins on the gyroscope, ST1 and ST2. When applying a logic 1 to ST1, the output voltage of the sensor should typically drop 660 mV. It can range from 400 to 1000 mV. When applying a logic 1 to ST2, the voltage should increase by the same amount and have the same range. A logic 1 is defined as a minimum of 3.3 V and a logic 0 is a maximum of 1.7 V. The following table shows the results of this test:

Self Test 1	
Logic Low:	2.57 V
Logic High:	1.87 V
Difference:	-.7 V
Self Test 2	
Logic Low:	2.57 V
Logic High:	3.35 V
Difference:	.78 V

Table 14: Gyroscope Self Test

Self test 1 produced a change of $-.7$ V and self test 2 produced a change of $.78$ V. Both of these values fall within the specifications of the sensor.

7 Conclusions

These tests conclude that these sensors although they do perform according to most of their specifications, are not able to produce accurate results in an inertial navigation system. A more accurate method for determining the bias of the sensors is needed. This would lead to more accurate positioning since the system would be able to determine whether acceleration is positive or negative based on a precise bias. A method for determining when the system is stationary would also be extremely useful. With the high noise that is currently being measured it is difficult for the system to conclude when it is stationary. One method to determine zero movement is through user intervention. When the user knows the system is stationary they could press a button alerting the system to recalibrate.

During the one –dimensional testing the final positioning varied from less than 1% error to well over 100%. It is impossible to tell when it is sensing movement

correctly until after the data is analyzed. From there it is possible to detect what is noise versus what acceleration is. Two-dimensional testing provided additional insight with a combination of all the sensors working together. Results from the 2-D testing exhibited a larger range of error from the prior tests. This could be due to more shock and vibrations from multiple changes in direction. This would cause the accelerometer and gyroscope to output incorrect values.

The noise in the signals is impossible to compensate for without losing resolution in the sensors. The noise is completely random - it can be both positive and negative and varies in magnitude. Each sensor has their own characteristics which make it very difficult to determine trends. The accelerometer had different characteristics within the X and Y axes. With this noise, calculated drift is impossible to overcome without being able to distinguish between noise and the actual signal. Noise reduction is needed for the sensors to be more reliable. Kalman filtering is a method that could be used to compensate for the noise in a system. This type of filtering is very complex and constantly adjusts to provide accurate information on the positioning of the system. Another method to account for noise is having redundant sensors. With additional sensors, if one of sensors has a spike on the output, but the others did not, the spike can be disregarded. Other filtering can increase accuracy in the system. When the project first started, a 4-point moving averager was implemented. However, due to the limited sampling rate, the averager was attenuating the applied accelerations more than it was attenuating the noise. This was taken out of the program sequence for that reason. With an increased sampling rate, this type of filtering can be implemented with greater benefits to reducing noise in the system.

With the current technology in MEMs accelerometers and gyroscopes, it is impossible to create an inertial navigation unit solely dependant on these sensors. The accuracy needed by a firefighter location device is much smaller than the amount that the current sensors can produce. They can be used in conjunction with different technologies such as GPS or digital compasses.

For future analysis of the MEMs sensors, it would require a processor that can gather data at a faster rate. Currently taking data at 6 samples per second is not fast enough to do much filtering to distinguish between noise and actual sensor information.

The 10-bit resolution of the analog to digital converters was a limiting factor because it did not provide enough resolution to see small amounts of drift. With a higher bit resolution, there will be less round off error when converting the analog signal into a digital form. Since the data was being stored in an array in C++, there was a limit to how many data points could be sampled. In order to monitor drift, the system needs to be able to gather data for at least 15 minutes to see the overall characteristics of drift.

A current method of reducing the effects of drift is to recalibrate often. This is a difficult technique to implement because the system must be stationary to recalibrate. It is not possible to rely on the system to know when it is stationary. Although the idea is simple, the implementation is not. Thermal drift in the gyroscope can be diminished if outputs from the temperature sensor are used. With a temperature sensor already installed on the gyroscope, the means to detect temperature fluctuations is already possible. However, as noted earlier by recalibrating after approximately 8 seconds a higher accuracy of final position is calculated.

This project provided a great introduction to the use of low cost MEMs technology in inertial navigation. The final deliverables include an inertial measurement unit that uses a two-axis accelerometer and a gyroscope. The system is capable of storing the data from the sensors and processing it to calculate the final positioning. It was also designed to be compatible with any accelerometer and gyroscope with an analog output. Although the accuracy was less than ideal due to reasons explained earlier, this project was beneficial to gain insight into the developing MEMs technology.

8 References

- ¹ U.S. Fire Administration - <http://www.usfa.dhs.gov/statistics/quickstats/>
- ² " navigation ." Encyclopedia Britannica 2006. Encyclopedia Britannica Online. 17 Sep. 2006
<http://search.eb.com/eb/article-61195>
- ³ Andrews Space and Technology. http://www.spaceandtech.com/spacedata/constellations/navstar-gps_consum.shtml 20 Sep. 2006
- ⁴ Stansell, Thomas A. Jr. "GPS Modernization" in AccessScience@McGraw-Hill, <http://www.accessscience.com>, 18 Sep. 2006
- ⁵ Shuurman, Nadine. GIScience at SFU. http://www.sfu.ca/gis/bguides/icons/fig3_1_GPS.gif 21 Sep. 2006
- ⁶ " navigation ." Encyclopedia Britannica 2006. Encyclopedia Britannica Online. 17 Sep. 2006
<http://search.eb.com/eb/article-61195>
<http://search.eb.com/eb/article-61165>
- ⁷ Kallahar "Resources for GPS Guided Robots," Gpsbots.com 1 Oct. 2006
- ⁸ Moody, Alton B. "Dead Reckoning" in AccessScience@McGraw-Hill, <http://www.accessscience.com>, 18 Sep. 2006
- ⁹ Intel Corporation - <http://www.intel.com/technology/comms/uwb/>
- ¹⁰ Heller, Arnie. "Exploring the Ultra-Wideband" - <http://www.llnl.gov/str/September04/Azevedo.html>
- ¹¹ Heller, Arnie "Exploring the Ultra-Wideband" - <http://www.llnl.gov/str/September04/Azevedo.html>
- ¹² Nekoogar, Faranak - "Introduction to Ultra-Wideband Communication" - <http://www.phptr.com/articles/article.asp?p=433381&seqNum=5&rl=1>
- ¹³ Solenoid - <http://resources.schoolscience.co.uk/CDA/11-14/physics/copch33pg2.html>
- ¹⁴ Directional Antenna - http://en.wikipedia.org/wiki/Directional_antenna
- ¹⁵ Howell, William E. "Inertial Guidance System" in AccessScience@McGraw-Hill, <http://www.accessscience.com>, 18 Sep. 2006
- ¹⁶ Luethi, Peter. Thomas Moser "Low Cost Inertial Navigation System" <http://www.electronic-engineering.ch/study/ins/ins.html> 17 Sep. 2006
- ¹⁷ Analog Devices.
<http://www.analog.com/en/subCat/0,2879,764%255F800%255F0%255F0%255F0%255F00.html> 18 Sep 2006
- ¹⁸ "Gyroscope" (<http://www.answers.com/topic/gyroscope>) 19 Sep. 2006
- ¹⁹ Barbour, Neil. "Gyroscope" in AccessScience@McGraw-Hill, <http://www.accessscience.com>, 18 Sep. 2006
- ²⁰ <http://hyperphysics.phy-astr.gsu.edu/HBASE/imgmec/gyro.gif> 23 Sep. 2006
- ²¹ Barbour, Neil. "Gyroscope" in AccessScience@McGraw-Hill, <http://www.accessscience.com>, 18 Sep. 2006
- ²² Barbour, Neil. "Gyroscope" in AccessScience@McGraw-Hill, <http://www.accessscience.com>, 18 Sep. 2006
- ²³ Barbour, Neil. "Gyroscope" in AccessScience@McGraw-Hill, <http://www.accessscience.com>, 18 Sep. 2006
- ²⁴ Barbour, Neil. "Gyroscope" in AccessScience@McGraw-Hill, <http://www.accessscience.com>, 18 Sep. 2006
- ²⁵ "MEMS Gyroscopes Making Strides in Replacing Entrenched Technologies"
<http://www.instat.com/press.asp?ID=827&sku=IN030884EA> 25 Sep. 2006
- ²⁶ McLellan, J. Mac. "Low-Cost Solid State Gyro Approved"
http://www.flyingmag.com/article.asp?section_id=17&article_id=265 23 Sep. 2006
- ²⁷ Green, John, David Krakauer. "New iMEMs Angular-Rate-Sensing Gyroscope"
<http://www.analog.com/library/analogdialogue/archives/37-03/gyro.html> 20 Sep. 2006
- ²⁸ Green, John, David Krakauer. "New iMEMs Angular-Rate-Sensing Gyroscope"
<http://www.analog.com/library/analogdialogue/archives/37-03/gyro.html> 20 Sep. 2006
<http://www.analog.com/library/analogdialogue/archives/37-03/gyro.html>
- ²⁹ "ADXRS150" http://www.analog.com/UploadedFiles/Data_Sheets/ADXRS150.pdf

-
- ³⁰ “iMEMS Gyroscopes”
<http://www.analog.com/en/subCat/0,2879,764%255F801%255F0%255F%255F0%255F,00.html> 27 Sep. 2006
- ³¹ Korvink, Jan G & Oliver Paul. “MEMS – a practical guide to design, analysis and applications.” William Andrew Inc. 2006. Pg. 17
- ³² <http://www.Gumstix.com/about.html>
- ³³ Swett, Sam. “Digital Cameral Memory Cards” http://plex.us/outbursts/dc_memory.html 1 Oct. 2006
- ³⁴ “Not Sure Which Memory You Need?” <http://www.crucial.com/index.asp> 1 Oct. 2006
- ³⁵ “ADXL103/ADXL203” http://www.analog.com/UploadedFiles/Data_Sheets/ADXL103_203.pdf
- ³⁶ “ADXL103/ADXL203” http://www.analog.com/UploadedFiles/Data_Sheets/ADXL103_203.pdf
- ³⁷ “ADXL203EB”
http://www.analog.com/UploadedFiles/Evaluation_Boards_Tools/535395787ADXL203EB_0.pdf
- ³⁸ “ADXRS150” http://www.analog.com/UploadedFiles/Data_Sheets/ADXRS150.pdf
- ³⁹ “ADXRS150EB”
http://www.analog.com/UploadedFiles/Evaluation_Boards/Tools/9303074ADXRS150EB_0.pdf
- ⁴⁰ “SR50 Series Compact High Resolution Rotation Stages”
<http://www.newport.com/store/genproduct.aspx?id=140164&lang=1033&Section=Spec> 14 Feb. 2007
- ⁴¹ http://www.analog.com/UploadedFiles/Data_Sheets/ADXRS150.pdf 16 April. 2007

Appendix A: ADXRS150 Specifications

ADXRS150

SPECIFICATIONS

@T_A = 25°C, V_S = 5 V, bandwidth = 80 Hz (C_{OUT} = 0.01 μF), angular rate = 0°/s, ±1g, unless otherwise noted.

Table 1.

Parameter	Conditions	ADXRS150ABG			Unit
		Min ¹	Typ	Max ¹	
SENSITIVITY					
Dynamic Range ²	Clockwise rotation is positive output Full-scale range over specifications range	±150			°/s
Initial	@25°C	11.25	12.5	13.75	mV/°/s
Over Temperature ³	V _{CC} = 4.75 V to 5.25 V	11.25		13.75	mV/°/s
Nonlinearity	Best fit straight line		0.1		% of FS
Voltage Sensitivity	V _{CC} = 4.75 V to 5.25 V		0.7		%/V
NULL					
Initial Null			2.50		V
Null Drift over Temperature ³	Delta from 25°C			±300	mV
Turn-On Time	Power on to ±½°/s of final		35		ms
Linear Acceleration Effect	Any axis		0.2		°/s/g
Voltage Sensitivity	V _{CC} = 4.75 V to 5.25 V		1		°/s/V
NOISE PERFORMANCE					
Rate Noise Density	@25°C		0.05		°/s/√Hz
FREQUENCY RESPONSE					
3 db Bandwidth ⁴ (User Selectable)	22 nF as comp cap (see the Applications section)		40		Hz
Sensor Resonant Frequency			14		kHz
SELF TEST					
ST1 RATEOUT Response ⁵	ST1 pin from Logic 0 to 1, -40°C to +85°C	-400	-660	-1000	mV
ST2 RATEOUT Response ⁵	ST2 pin from Logic 0 to 1, -40°C to +85°C	+400	+660	+1000	mV
Logic 1 Input Voltage	Standard high logic level definition	3.3			V
Logic 0 Input Voltage	Standard low logic level definition			1.7	V
Input Impedance	To common		50		kΩ
TEMPERATURE SENSOR					
V _{OUT} at 298°K			2.50		V
Max Current Load on Pin	Source to common			50	μA
Scale Factor	Proportional to absolute temperature		8.4		mV/°K
OUTPUT DRIVE CAPABILITY					
Output Voltage Swing	I _{OUT} = ±100 μA	0.25		V _S - 0.25	V
Capacitive Load Drive		1000			pF
2.5 V REFERENCE					
Voltage Value		2.45	2.5	2.55	V
Load Drive to Ground	Source		200		μA
Load Regulation	0 < I _{OUT} < 200 μA		5.0		mV/mA
Power Supply Rejection	4.75 V _S to 5.25 V _S		1.0		mV/V
Temperature Drift ³	Delta from 25°C		5.0		mV
POWER SUPPLY					
Operating Voltage Range		4.75	5.00	5.25	V
Quiescent Supply Current			6.0	8.0	mA
TEMPERATURE RANGE					
Specified Performance Grade A		-40		+85	°C

¹ All min and max specifications are guaranteed. Typical specifications are not tested or guaranteed.

² Dynamic range is the maximum full-scale measurement range possible, including output swing range, initial offset, sensitivity, offset drift, and sensitivity drift at 5 V supplies.

³ Specification refers to the maximum extent of this parameter as a worst-case value at T_{MIN} or T_{MAX}.

⁴ Frequency at which response is 3 dB down from dc response with specified compensation capacitor value. Internal pole forming resistor is 180 kΩ. See the Setting Bandwidth section.

⁵ Self-test response varies with temperature. See the Self-Test Function section for details.

Appendix B: ADXL203 Specifications

ADXL103/ADXL203

SPECIFICATIONS

$T_A = -40^{\circ}\text{C}$ to $+125^{\circ}\text{C}$, $V_S = 5\text{ V}$, $C_X = C_Y = 0.1\ \mu\text{F}$, acceleration = 0 g , unless otherwise noted.

Table 1.

Parameter	Conditions	Min ¹	Typ	Max ²	Unit
SENSOR INPUT	Each axis				
Measurement Range ²		± 1.7			g
Nonlinearity	% of full scale		± 0.2	± 1.25	%
Package Alignment Error			± 1		Degrees
Alignment Error (ADXL203)	X sensor to Y sensor		± 0.1		Degrees
Cross-Axis Sensitivity			± 1.5	± 3	%
SENSITIVITY (RATIOMETRIC)³	Each axis				
Sensitivity at X_{out} , Y_{out}	$V_S = 5\text{ V}$	960	1000	1040	mV/g
Sensitivity Change Due to Temperature ⁴	$V_S = 5\text{ V}$		± 0.3		%
ZERO g BIAS LEVEL (RATIOMETRIC)	Each axis				
0 g Voltage at X_{out} , Y_{out}	$V_S = 5\text{ V}$	2.4	2.5	2.6	V
Initial 0 g Output Deviation from Ideal	$V_S = 5\text{ V}$, 25°C		± 25		mg
0 g Offset vs. Temperature			± 0.1	± 0.8	mg/ $^{\circ}\text{C}$
NOISE PERFORMANCE					
Output Noise	$<4\text{ kHz}$, $V_S = 5\text{ V}$		1	3	mV rms
Noise Density			110		$\mu\text{g}/\sqrt{\text{Hz}}$ rms
FREQUENCY RESPONSE⁵					
C_X , C_Y Range ⁶		0.002		10	μF
R _{int} Tolerance		24	32	40	k Ω
Sensor Resonant Frequency			5.5		kHz
SELF TEST⁷					
Logic Input Low				1	V
Logic Input High		4			V
ST Input Resistance to Ground		30	50		k Ω
Output Change at X_{out} , Y_{out}	Self Test 0 to Self Test 1	450	750	1100	mV
OUTPUT AMPLIFIER					
Output Swing Low	No load	0.05	0.2		V
Output Swing High	No load		4.5	4.8	V
POWER SUPPLY					
Operating Voltage Range		3		6	V
Quiescent Supply Current			0.7	1.1	mA
Turn-On Time ⁸			20		ms

¹ All minimum and maximum specifications are guaranteed. Typical specifications are not guaranteed.

² Guaranteed by measurement of initial offset and sensitivity.

³ Sensitivity is essentially ratiometric to V_S . For $V_S = 4.75\text{ V}$ to 5.25 V , sensitivity is 186 mV/W/g to 215 mV/W/g.

⁴ Defined as the output change from ambient-to-maximum temperature or ambient-to-minimum temperature.

⁵ Actual frequency response controlled by user-supplied external capacitor (C_X , C_Y).

⁶ Bandwidth = $1/(2 \times \pi \times 32\text{ k}\Omega \times C)$. For C_X , $C_Y = 0.002\ \mu\text{F}$, bandwidth = 2500 Hz. For C_X , $C_Y = 10\ \mu\text{F}$, bandwidth = 0.5 Hz. Minimum/maximum values are not tested.

⁷ Self-test response changes cubically with V_S .

⁸ Larger values of C_X , C_Y increase turn-on time. Turn-on time is approximately $160 \times C_X$ or $C_Y + 4\text{ ms}$, where C_X , C_Y are in μF .